



## Eruptive history of Chimborazo volcano (Ecuador): A large, ice-capped and hazardous compound volcano in the Northern Andes

Pablo Samaniego<sup>a,b,c,d,\*</sup>, Diego Barba<sup>d</sup>, Claude Robin<sup>a,b,c,d</sup>, Michel Fornari<sup>e</sup>, Benjamin Bernard<sup>c,d,f</sup>

<sup>a</sup> Clermont Université, Université Blaise Pascal, Laboratoire Magmas et Volcans, BP 10448, F-63000 Clermont-Ferrand, France

<sup>b</sup> CNRS, UMR 6524, Laboratoire Magmas et Volcans, 5 rue Kessler, 63038 Clermont-Ferrand cedex, France

<sup>c</sup> IRD, R 163, Laboratoire Magmas et Volcans, 5 rue Kessler, 63038 Clermont-Ferrand cedex, France

<sup>d</sup> Instituto Geofísico, Escuela Politécnica Nacional, Ap. 17-01-2759, Quito, Ecuador

<sup>e</sup> IRD, UMR Géosciences Azur, Université Nice-Sophia Antipolis, Parc Valrose, 06108 Nice, France

<sup>f</sup> Universidad San Francisco de Quito, Diego de Robles y vía Interoceánica, Quito, Ecuador

### ARTICLE INFO

#### Article history:

Received 24 August 2011

Accepted 30 January 2012

Available online 8 February 2012

#### Keywords:

Chimborazo

Andean volcanism

Late Pleistocene

Eruptive rates

Volcanic hazards

<sup>40</sup>Ar–<sup>39</sup>Ar geochronology

### ABSTRACT

New fieldwork, radiometric and whole-rock chemical data permit the reconstruction of the main eruptive stages of the Chimborazo compound volcano, the highest summit of the Northern Andes. Chimborazo is composed of three successive edifices. The Basal Edifice (CH-I) was active from ~120 to 60 ka and resulted in a large, mostly effusive edifice which was built up during two stages of cone-building, terminating with the formation of a dome complex. This edifice was affected by a huge sector collapse around 65–60 ka which produced a major debris avalanche that spread out into the Riobamba basin, covering about 280 km<sup>2</sup> with an average thickness of 40 m and a total volume of ~10–12 km<sup>3</sup>. After the emplacement of the Riobamba debris avalanche, eruptive activity resumed at the eastern outlet of the avalanche scar and was responsible for the construction of a less voluminous, Intermediary Edifice (CH-II), whose current remnants are the Politécnica and Martínez peaks. This edifice developed from 60 to 35 ka. Lastly, eruptive activity shifted to the west, leading to the construction of the morphologically well-preserved Young Cone (CH-III) which currently forms the highest summit (Whymper).

The average eruptive rate of Chimborazo volcano is 0.5–0.7 km<sup>3</sup>/ka. However, looking at the three successive edifices individually, we estimate that there has been a progressive decrease in magma output rate from the Basal Edifice (0.7–1.0 km<sup>3</sup>/ka), through the Intermediary Edifice (0.4–0.7 km<sup>3</sup>/ka) to the Young Cone (~0.1 km<sup>3</sup>/ka). However, during the main cone-building stages, the peak eruption rates are markedly higher, indicating significant variations in the magma output rate during the lifespan of this arc volcano. During the Holocene, the Chimborazo eruptive activity consisted of small-volume explosive events that occurred at quite regular intervals, between about 8000 and 1000 yr ago. Since the last eruption occurred between the early part of the 5th century and the end of the 7th century, and the average time interval between the events is about 1000 yr, Chimborazo must be considered as a potentially active volcano. The presence of a thick ice cap covering the summit, its steep flanks and its position above the populated lowland area of Riobamba and Ambato, are factors that result in a high potential risk.

© 2012 Elsevier B.V. All rights reserved.

### 1. Introduction

In Ecuador, the volcanoes related to the subduction of the Nazca Plate are distributed along two 300 km-long volcanic alignments, with a subordinate back-arc province (Fig. 1). The volcanic front is situated along the Western Cordillera of the Ecuadorian Andes, whereas the main arc is 35–60 km behind the front, defining a second,

quite disperse alignment, lying in the Eastern Cordillera and the tectonic depression between the two cordilleras (the Inter Andean Valley). The volcanic front mainly consists of dacitic volcanic centres, and includes the historically active Pichincha volcano, as well as the potentially active Cuicocha, Imbabura, Pululhua, Atacazo, Illiniza, and Quilotoa volcanic centres. In contrast, the main arc consists of andesitic stratocones, the most important being the large, ice-clad and active Cayambe, Antisana, Cotopaxi, Tungurahua, and Sangay volcanoes (Hall et al., 2008).

Chimborazo volcano (01°30'S, 78°36'W, 6268 m above sea level-asl-), located 150 km south of Quito, is the highest peak of the Northern Andes (Fig. 1a). It is constructed on the Western Cordillera, in the southern part of the Ecuadorian volcanic province. Chimborazo volcano, and its

\* Corresponding author at: IRD, Casilla 18-1209, Calle Teruel 357, Miraflores, Lima 18, Peru.

E-mail address: [pablo.samaniego@ird.fr](mailto:pablo.samaniego@ird.fr) (P. Samaniego).

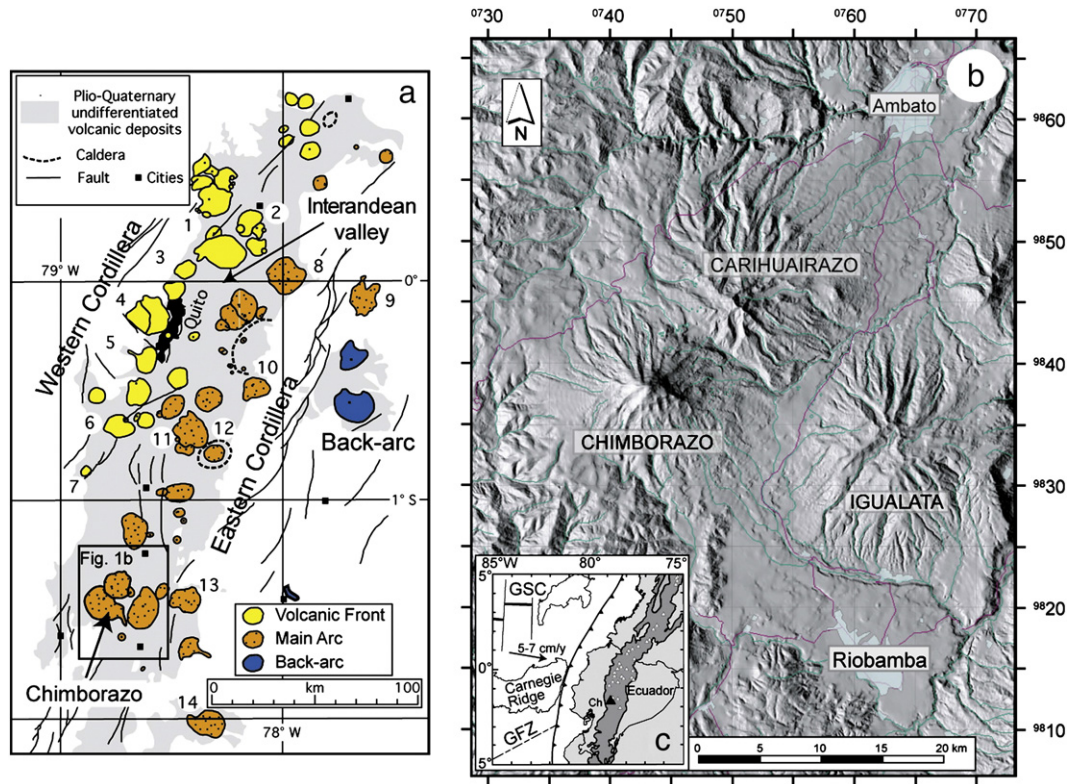


**Fig. 1.** (a) The Ecuadorian volcanic arc. Main volcanoes: (1) Cuicocha; (2) Imbabura; (3) Pululhua; (4) Pichincha; (5) Atacazo-Ninahuilca; (6) Ilinizas; (7) Quilotoa; (8) Cayambe; (9) El Reventador; (10) Antisana; (11) Cotopaxi; (12) Chalupas caldera; (13) Tungurahua; (14) Sangay. (b) Digital elevation model showing the Chimborazo and Carihuairazo volcanic group and the adjacent Ambato and Riobamba basins. (c) Geodynamic setting of the Ecuadorian arc, including main oceanic features. Andes range defined by 2000 m contour line. Trench is defined by a toothed line and active volcanoes by open triangles. Black arrow is the direction of subduction. GSC: Galápagos Spreading Centre; GFZ: Grijalva Fracture Zone; Ch: Chimborazo volcano.

neighbours Carihuairazo and Igualata volcanoes, stand out to form a high relief between the Ambato and Riobamba tectonic depressions that form the southern part of the Inter Andean Valley (Fig. 1b). Since the 18th century most travellers, naturalists, and geologists have been fascinated by the magnificence of Chimborazo, which is notable for its relief (2000–3000 m), steep flanks, and its large glacier cap. Early descriptions of Chimborazo were done by Humboldt (1837–1838), Whymper (1892), Meyer (1907), Reiss and Stübel (1892), and Sauer (1971). The first “modern” geological studies of Chimborazo volcano were carried out by Kilian (1987), Beate and Hall (1989), and Kilian et al. (1995), who studied the volcanic stratigraphy, structure and petrology of Chimborazo volcanic rocks. In addition, Clapperton and Smith (1986) and Clapperton (1990) studied the geomorphology of the Chimborazo–Carihuairazo massif, in relation to the glacial and volcanic activity, and gave the first description of a huge debris avalanche, originated from the Chimborazo volcano and that spread out within the Riobamba basin (Fig. 1b). Despite the fact that the volcano has not shown any eruptive activity since the arrival of the Spaniards (in the first half of the 16th century), its “young” morphology suggest that it is potentially active, and a volcanic hazard map was also published (Beate et al., 1990). In spite of all these works, no consensus existed concerning the structure of the volcano, as well as the absolute time span of its development. More recently, in the framework of an Ecuadorian–French research programme, we started a comprehensive study of this volcano. We have published a detailed description of the Chimborazo debris avalanche (Alcaraz, 2002; Bernard et al., 2008), and described, for the first time, the recurrent explosive activity from ~8000 to 1000 years before present (yr BP), corroborating the active nature of the volcano (Barba et al., 2008). Glacial retreat during the last few years has enabled new field observations, which are combined with geochronological and petrological data to reconstruct

the volcanic history and structure of Chimborazo volcano since the Late Pleistocene.

## 2. Methodology

Fieldwork was carried out during several high-altitude field trips between 2004 and 2006, which includes geological mapping and sampling of most volcanic units. Steep topography on the upper flanks of the volcano, the presence of a large ice cap, and the voluminous glacial deposits around the cone made it difficult to carry out an exhaustive sampling of all the volcanic units (specially on the southeast flank). However, the presence of deep, U-shaped, radially-oriented glacial valleys enabled the main volcanic units to be studied (Fig. 2), resulting in extensive sampling for petrographic and major and trace element studies (Fig. 3). This work is based on more than twenty detailed stratigraphic sections on distal tephra fallout deposits (nine of which are presented here). Major and trace element analyses were obtained for agate-crushed powders of 192 samples from the whole edifice, using an Inductive Coupled Plasma-Atomic Emission Spectrometer (ICP-AES) at the Laboratoire Domaines Océaniques, Université de Bretagne Occidentale (Brest, France). These data, together with petrographic descriptions of thin sections, are used to characterize and correlate the different volcanic units.

Fifteen lavas (including 4 samples from the nearby Carihuairazo volcano) have been dated using the  $^{40}\text{Ar}$ – $^{39}\text{Ar}$  method (on hand-picked fragments from the matrix) at the Geochronology Laboratory at Géosciences Azur, University of Nice (France). The criteria for defining a “plateau” age are the following: (1) it must contain at least 60% of the total  $^{39}\text{Ar}$  released; (2) there must be at least three successive step-heating fractions in the plateau; and (3) the integrated age of the plateau (weighted average of apparent ages of individual fractions

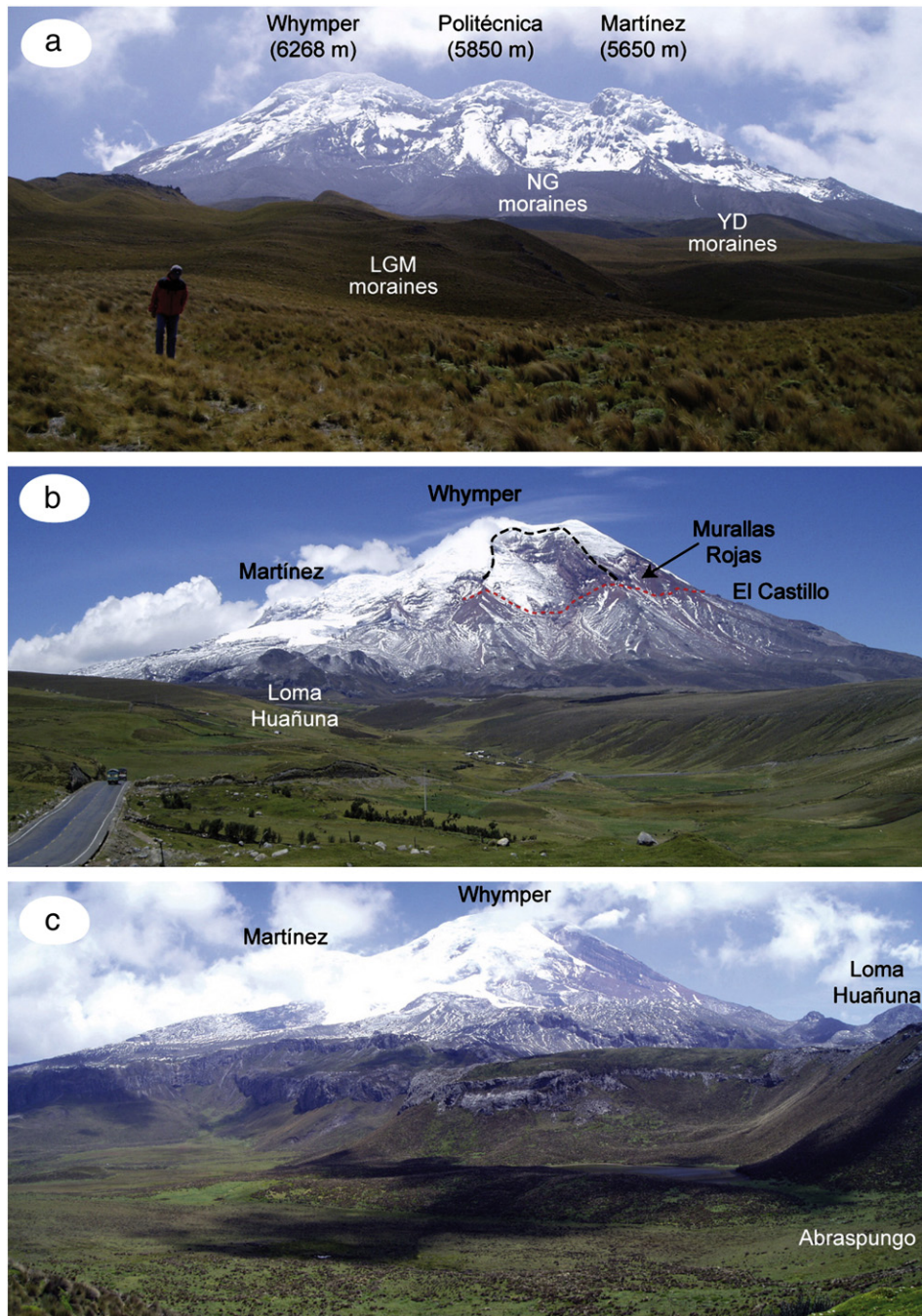


**Fig. 2.** Panoramic views of the Chimborazo volcano. (a) View from the south showing the three summits, and in the foreground, the Last Glacial Maximum (LGM), Younger Dryas (YD) and Neo-Glacial (NG) moraines. (b) View from the Ambato-Guaranda road, showing the older lava flows of the basal volcano (Loma Huañuna), the lavas of the El Castillo, as well as the younger cone and the Whympier summit. Also marked are the caldera scar (lower dashed line) and younger flank collapse scar affecting the main summit (upper dashed line). (c) North-east flank of Chimborazo, showing the older lavas (Loma Huañuna and Abraspungo) as well as the younger lavas of the main edifice.

comprising the plateau) must lie within a 2 sigma error of each apparent age of the plateau. Ages were obtained from measured isotope ratios, which had been corrected for mass fractionation, system blanks, and interfering isotopes produced during irradiation. Isochron ages were calculated using a reverse isochron diagram of  $^{36}\text{Ar}/^{40}\text{Ar}$  vs.  $^{39}\text{Ar}/^{40}\text{Ar}$ , using the least squares method. Results are presented in Table 1. The Late Pleistocene chronology was completed by two  $^{14}\text{C}$  dates carried out at the Centre for Isotope Research, University of Groningen, Netherlands, both by the conventional and the Accelerator Mass Spectrometry (AMS) methods.

### 3. Morphology and structure

#### 3.1. Morphology and glacial history

Chimborazo volcano has an elliptical shape (14 km N–S by 20 km E–W) and an unusual relief characterized by three main peaks, roughly aligned WNW–ESE (Figs. 1, 2). The highest point of the volcano is the “Whympier” summit (6268 m asl), whereas the two other peaks, the “Politécnica” and “Martínez”, reach 5850 and 5650 m asl, respectively, and are located eastward at 1.25 and 2.25 km from the main summit.

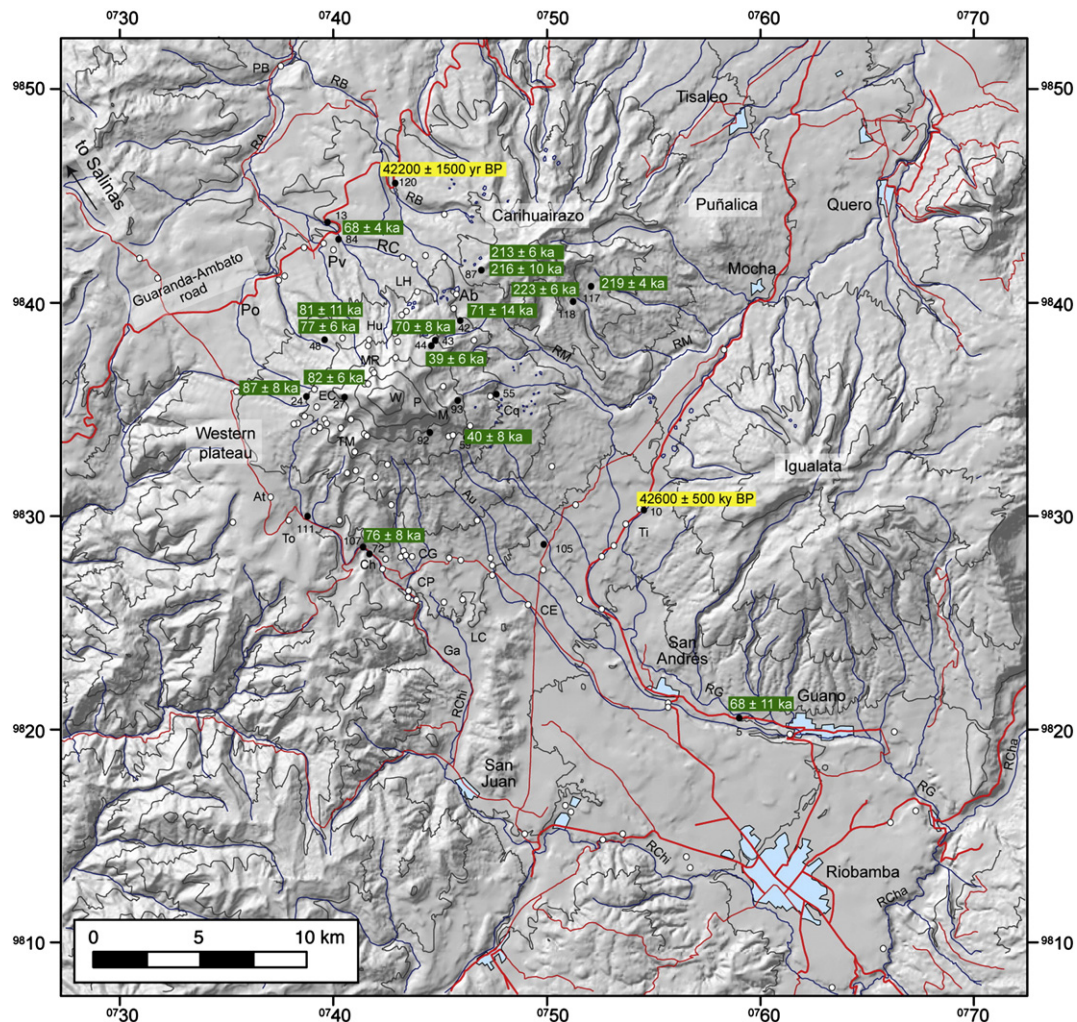


**Fig. 3.** Digital elevation model of the Chimborazo volcano showing locations of samples (open circles) and studied sections (solid circles).  $^{40}\text{Ar}/^{39}\text{Ar}$  and  $^{14}\text{C}$  ages obtained during this study are also included. W, Whympet summit; P, Politécnica peak; M, Martínez peak; Cq, Chuquipogoyos; Ti, Tintatacto; RG, Río Guano; RCha, Río Chambo; RChi, Río Chimborazo; CE, Cuatro Esquinas; Ga, Gabín; CP, Condor Palta; CG, Culebrilla Grande; Au, Aucacán; Ch, Chorrera; To, Totorillas; At, Atacruz; TM, Templo Machay; EC, El Castillo; Po, Potrerillos; Pv, Polvoloma; Hu; Huayhuaycu; MR, Murallas Rojas; RC, Río Colorado; RB, Río Blanco; RA, Río Ambato; PB, Peñas Blancas; Ab, Abraspungo; LH, Loma Huañuna; RM, Río Mocha.

From the upper flanks, glaciers extend down to 4800–5000 m on the more humid eastern and northeastern sides, whereas they only reach down to 5500–6000 m on the drier, western side (Fig. 2). Chimborazo reaches ~2400 m in height on the north and west sides, and ~2800–3000 m on the steeper southeast side. This difference is due to several factors: the presence of the older Carihuairazo volcano, located to the northeast of Chimborazo; the morphology of the substratum, which displays higher elevations to the north and west of the volcano; and the location of the Riobamba depression to the southeast of Chimborazo (Fig. 3). The location and subsequent evolution of the volcano was controlled by regional Andean-trending faults, the most important being the “Pallatanga” fault system (Winter et al., 1993), whose surface expression has been mapped several kilometres to the south and southwest of Chimborazo. The volcano lies on Cretaceous oceanic-plateau basalts and Cenozoic volcano-sedimentary sequences, which are overlain by Mio-Pliocene volcanic arc sequences (McCourt et al., 1997; Hughes and Pilatasig, 2002).

The morphology of Chimborazo has been greatly influenced by the late Pleistocene glaciations. Major glacial valleys have been carved around the cone, and large quantities of moraine deposits were stacked at the foot of the volcano. The Chimborazo and Carihuairazo volcanoes, and notably the Río Mocha valley between these volcanoes, have been the focus of several glaciological and geomorphological

studies aimed to constrain the timing and magnitude of Late Pleistocene glaciations in this part of the Andes (Clapperton and McEwan, 1985; Clapperton, 1990; Heine, 1993; Rodbell and Seltzer, 2000). Here, Clapperton and McEwan (1985) identified three groups of moraines that were assigned to Last Glacial Maximum (LGM), Younger Dryas (YD), and Neo-Glacial (NG) periods. The older moraines extend down to 3500–3600 m around the cone, and are recognized on the north, east, and south flanks. These glacial deposits generally consist of three to four small, inner moraines (5–10 m high) within 100–200 m-high outer moraines. These moraines are covered by several metres of reworked and partially altered ash (locally named “cangahua”) and paleosols. A maximum age ( $33,290 \pm 300$  yr BP) is obtained on a peat layer underlying a till on the northeast flank of Carihuairazo, which is correlated with this group of moraines. The minimum age ( $14,770 \pm 60$  yr BP) was obtained from a peat horizon inter-layered with a sequence of glacial sediments, associated with the outer moraines in the Río Mocha valley. Based on these age constraints, and by analogy with other regions of the Northern Andes, Clapperton (1990) linked this group of moraines to the LGM period, dated at between ca. 33 and 14 ka.

The intermediate sequence of moraines are radially distributed around the Chimborazo cone and are characterized by forming a group of three to four arcuate terminal moraines reaching

**Table 1**  
<sup>40</sup>Ar–<sup>39</sup>Ar ages for rocks from Chimborazo volcano.

Sample number	Lab number	Edifice	Rock type and location	UTM coordinate <sup>a</sup> East–North	Plateau age ± 2 s	<sup>39</sup> Ar <sup>b</sup>	Isochrone age ± 2 s	Ri <sup>c</sup>	MSWD <sup>d</sup>
CH-DB-44	M1797	Intermediary Edifice	Lava flow, ESE flank, below Martínez summit	07,451–98,406	37 ± 9	75%	39 ± 6	294.7 ± 0.9	1.8
CH-DB-59	M1847	Intermediary Edifice	Lava flow, ESE flank, below Martínez summit	07,467–98,362	40 ± 8	77%	40 ± 8	295.6 ± 0.8	1.7
RIO-5	K366	Intermediary Edifice	Guano lava flow	07,598–98,231	60 ± 11	94%	68 ± 10	292.3 ± 2.8	0.4
RIO-84	M1848	Basal Edifice	Lava flow, NW flank, Polvoloma	07,407–98,455	68 ± 6	88%	68 ± 4	294.6 ± 0.7	0.8
CH-DB-43	M1851	Basal Edifice	Lava flow, NE flank	07,452–98,407	74 ± 8	80%	70 ± 8	297.5 ± 1.0	1.2
CH-DB-42	M1722	Basal Edifice	Lava flow, NE flank, Abraspungo	07,464–98,414	87 ± 27	81%	71 ± 14	296.6 ± 0.8	1.8
RIO-72	M1822	Basal Edifice	Lava flow, W flank, Chorrera	07,422–98,308	77 ± 8	86%	76 ± 8	296.1 ± 2.0	1.3
CH-DB-48A	M1876	Basal Edifice	Lava flow, NW flank	07,400–98,408	82 ± 8	85%	77 ± 6	296.9 ± 1.1	0.6
CH-DB-48B	M1796	Basal Edifice	Lava flow, NW flank	07,400–98,408	80 ± 8	53%	81 ± 11	294.1 ± 1.7	2.5
CH-DB-27	M1757	Basal Edifice	Lava flow, W flank, El Castillo	07,410–98,381	83 ± 7	77%	82 ± 6	293.0 ± 1.9	0.8
CH-DB-24	M1845	Basal Edifice	Lava flow, W flank, El Castillo	07,393–98,382	87 ± 15	88%	87 ± 8	295.3 ± 0.7	0.4
RIO-87A	M2042	Carihuairazo	Lava flow, SW flank	07,473–98,441	213 ± 5	65%	213 ± 6	291.5 ± 1.2	2.5
RIO-87B	M2001	Carihuairazo	Lava flow, SW flank	07,473–98,441	208 ± 10	85%	216 ± 10	292.4 ± 1.2	1.6
RIO-117	M2000	Carihuairazo	Lava flow, SE flank	07,545–98,414	221 ± 5	89%	219 ± 4	298.0 ± 1.4	1.2
RIO-118	M2010	Carihuairazo	Lava flow, SE flank	07,518–98,410	224 ± 5	91%	223 ± 6	295.2 ± 1.4	1.5

<sup>a</sup> Location samples are given to 100 m using the UTM metric grid (1956, Provisional South America, zone 17), which is shown on Instituto Geográfico Militar maps.

<sup>b</sup> Percentage of total <sup>39</sup>Ar included in the plateau age.

<sup>c</sup> (<sup>40</sup>Ar/<sup>36</sup>Ar) initial ratio.

<sup>d</sup> Mean square of weighted deviations.

3900–4050 m down into the Rio Mocha valley (and other valleys of the eastern half of the volcano), and only 4300–4400 m on the drier, western flank. This group of moraines is dated by analysing peat horizons inter-layered with lake sediments associated with moraines of this group in the Rio Mocha valley. These samples yield uncalibrated ages of around 10–12 ka (11,370 ± 60 yr BP and 10,650 ± 60 yr BP; Clapperton and McEwan, 1985). Based on these ages Clapperton (1990) suggests that they correspond to the Younger Dryas cold climate event. This interpretation was challenged by Heine (1993), who dated the same peat layers, and obtained similar ages (10,975 ± 85 and 10,620 ± 85 yr BP). However, this author pointed out that the dated peat horizons are inter-layered within a 17–18 m-thick lake sediment sequence, implying that these ages are younger than the glacier advance responsible for moraine formation. Calculating the sedimentation rate for the 1.8 m-thick layer of sediments between the two dated peat horizons and using this sedimentation rate for the 8–9 m of sediments between the lower peat and the moraine, this author concluded that the moraines damming the valley pre-dated the YD event by at least 2500 yr (i.e. back to 13–15 ka). Based on these data and observations, Heine (1993), and more recently Rodbell and Seltzer (2000), challenged Clapperton's interpretation of a YD glacier advance. Lastly, the younger group of massive moraines is also radially distributed around the cone, and reach 4300–4400 m down into the Rio Mocha valley and 4600–4800 m on the western side of the cone. Clapperton (1990) proposed that this group of moraines may be ascribed to the Neo-Glacial period and formed by repeated glacier advances over the last 5 ka.

### 3.2. Overall structure

Previous reconstructions of Chimborazo's structure show a complex evolution, which is characterized by the development of several successive edifices (Kilian, 1987; Beate and Hall, 1989; Clapperton, 1990). These models are mainly based on morphological features, such as dip directions of lava flows, and the presence of angular unconformities between the volcanic sequences of the Chimborazo cone. On the western flank of the volcano there is a semi-circular structure (3–4 km in diameter) that extends from the northern to the southern flanks, at an altitude of around 5300–5400 m asl (Fig. 4a–c). This unconformity separates old lavas, corresponding to a basal edifice, from younger lavas of the Chimborazo summit. This structure has been interpreted as an explosion caldera that terminated the basal volcano history (Kilian, 1987; Beate and Hall, 1989). Based on its morphology,

and on stratigraphic observations (see below), we re-interpret this unconformity as an avalanche caldera that cut into the basal edifice. Another important unconformity is observed on the southern flank, below the saddle between the Whymper and Politécnica peaks (Fig. 2a). This unconformity separates old lava units associated with the Politécnica peak to the east from younger lavas emitted from the Whymper summit to the west. A third unconformity was observed in the eastern flank, below the Martínez peak. Here, lavas from the Politécnica peak underlie the thick lava pile forming the Martínez peak (Fig. 2a).

In summary, we propose that Chimborazo is a compound volcano that comprises: (1) a Basal Edifice (CH-I) whose relicts correspond to the old, radially-oriented lava flows; (2) an Intermediary Edifice (CH-II) which developed on the eastern flank of the former, and whose remnants are largely dissected by glacial erosion, and are represented by the Politécnica and Martínez peaks; and (3) a Young Cone (CH-III) which constitutes the highest Whymper summit.

## 4. Volcanic units

### 4.1. The Basal Edifice (CH-I)

This edifice was constructed to the southwest of the older and eroded Carihuairazo volcano (Fig. 5). The products of this edifice are represented by two thick sequences of lava flows, two notable pyroclastic flow units, and the Riobamba debris avalanche deposit (Table 2).

#### 4.1.1. Abraspungo stage

Remnants of this older unit consist of a 300–400 m-thick pile of massive lava flows observed around the north and northeast foot of the volcano (Fig. 2c), in the Abraspungo saddle and the Rio Mocha valley. These lavas are two-pyroxene andesites (57–61 wt.% SiO<sub>2</sub>) with a highly porphyritic texture (phenocrysts up to 6 mm in size). Thick, viscous lava flows, of amphibole-bearing siliceous andesite to dacite composition (63–64 wt.% SiO<sub>2</sub>), crop out with low slope angles (<10°), on the north flank of the cone. The most important of these flows is the Loma Huañuna lava flow located on the northern foot of the volcano. There are no radiometric ages for this unit, but these lava flows overlie Carihuairazo lavas, for which four consistent ages of 213–223 ka were obtained on samples from the southwest and southeast flanks of the cone (RIO-87A, RIO-87B, RIO-117, and RIO-118, Table 1, Fig. 3). On the other hand, the Abraspungo lavas are overlain

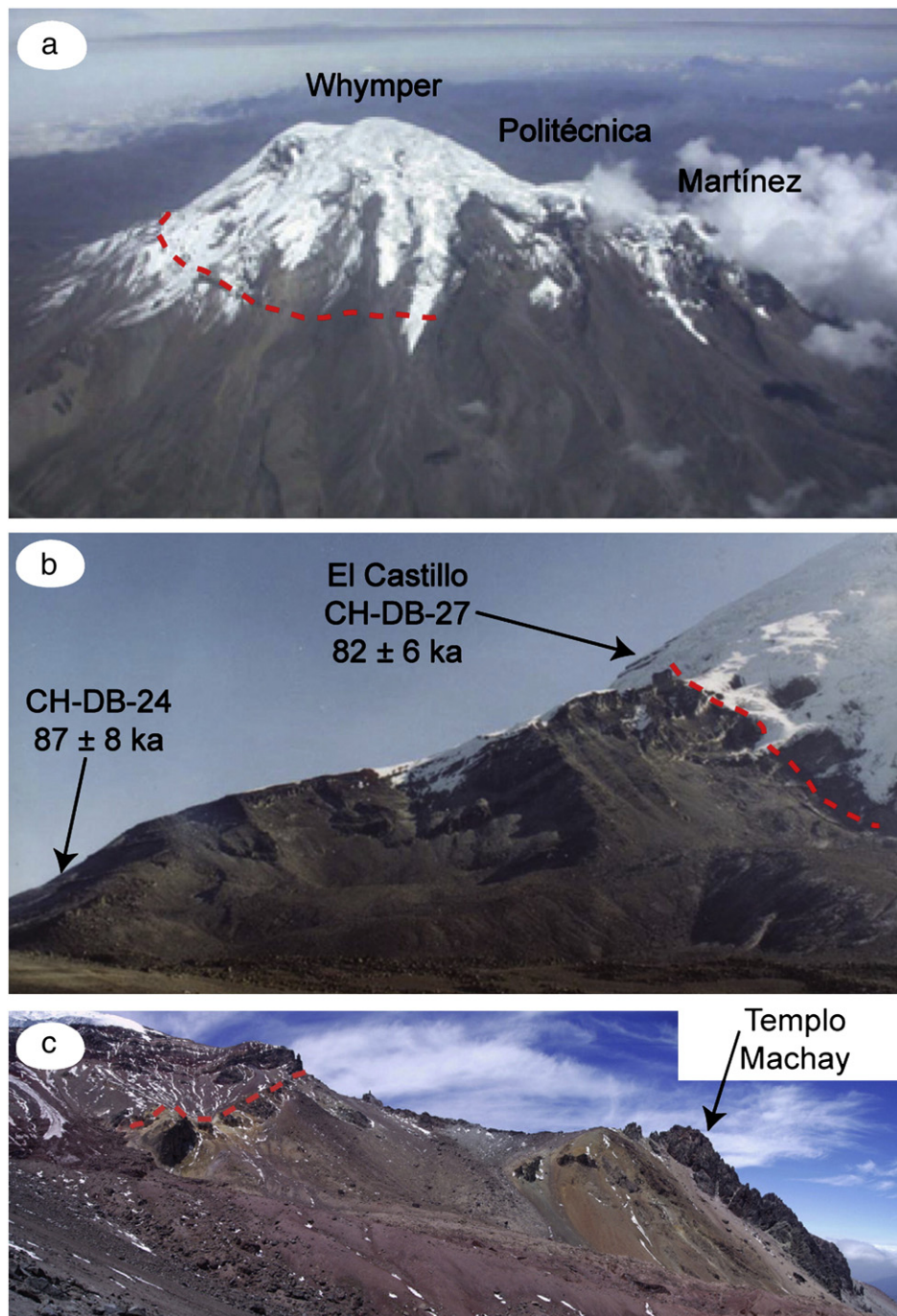


**Fig. 4.** Panoramic views of the west and southwest flanks of Chimborazo volcano. (a) Oblique view of Chimborazo volcano, showing the three main summits and the avalanche caldera scar. Photography kindly provided by P. Ramón (IGEPN). (b) View of the northwestern flank, showing the position of the two dated samples of the El Castillo section (CH-DB-24 and CH-DB-27), as well as the position of the avalanche caldera scar. (c) View of the southwestern flank, and the unconformity between the older lavas of the Templo Machay section and the younger lavas of the Main summit edifice.

by a second lava sequence (El Castillo stage), whose age is younger than 95 ka (see below). Thus, based on the stratigraphic position, its degree of erosion, and the previously mentioned chronological constraints, we propose a time span of ~120 to 100 ka for the Abraspungo lavas.

#### 4.1.2. El Castillo stage

This unit is represented by a sequence of lavas and subordinate breccias with a total thickness of at least 800 m and represents the main cone-building stage of the Basal Edifice (roughly corresponding to 70–80 vol.% of the whole basal volcano). The El Castillo lava flows rest unconformably on top of the older, sub-horizontal lavas of the

Abraspungo stage (Fig. 2c). This sequence gives the conical shape (15 to 25° dips) to the lower western and northern flanks of the Chimborazo cone. On the western side these lavas are observed on the lowermost slopes, at around 4600 m, and higher up where they form several topographically-distinct pinnacles around 5300–5400 m (e.g. “El Castillo”, Fig. 3b). On the eastern side they are observed lower down until 3500 m. The average extension of these lava flows is 7 to 8 km, although some flows, such as the Gabin lava flow, reach 14 km toward the south. Based on the radial distribution and dips of these lavas, we infer that the summit of the Basal Edifice was located at the same location as the present one, at an elevation of 6200 m asl.

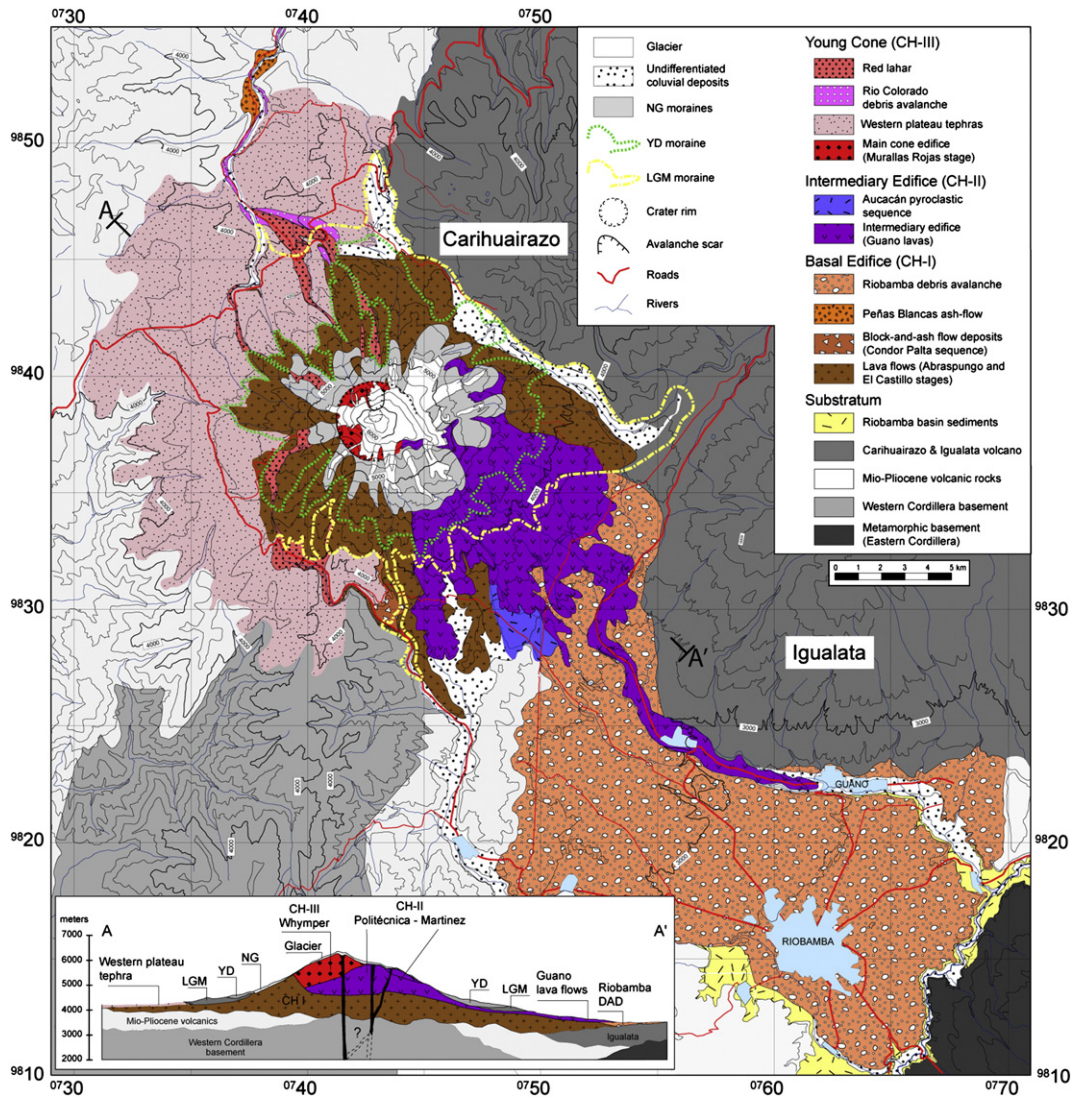


Fig. 5. Geological sketch map of Chimborazo volcano.

These lavas are mostly two-pyroxene andesites (57–60 wt.% SiO<sub>2</sub>), with rare amphibole andesites at the top of the sequence. One such example is the Templo Machay lavas (Fig. 4c), located on the southwest flank of the cone, which represent a remarkable sub-unit characterized by thick, viscous lava flows of amphibole-bearing siliceous andesitic and dacitic compositions (59–64 wt.% SiO<sub>2</sub>).

Six samples from this unit were dated using the <sup>40</sup>Ar/<sup>39</sup>Ar method (Table 1, Fig. 3). Two samples from the El Castillo crest on the northwestern flank of the cone were dated at 87 ± 8 and 82 ± 6 ka (CH-DB-24 and CH-DB-27, Fig. 4b). Four consistent, slightly younger ages were obtained from the northeast flank (70 ± 8 ka, CH-DB-43), the northwestern flank (77 ± 6 and 81 ± 11 ka, CH-DB-48A and B), and from a thick lava flow on the southern flank, the Chorrera lava (76 ± 8 ka, RIO-72). Lastly, a distal lava, corresponding to the top of the stratigraphic sequence, gave an age of 68 ± 4 ka (RIO-84). Based on these ages, the time span of the El Castillo stage is constrained to between 95 and 65 ka.

**4.1.2.1. Peñas Blancas ashflow deposit.** A massive ash-and-pumice flow deposit, 50–60 m in thickness, crops out to the northwest of the cone, in the Río Colorado valley (Fig. 5). The deposit is massive, well-compacted, matrix-supported, with an ashy matrix, and common rounded pumice lapilli (~15 vol.%) and accidental clasts (5 vol.%), the latter deriving

from dense lavas from the conduit and the basement rocks. The pumice fragments (<10 cm) are whitish in colour and rhyolitic in composition (70 wt.% SiO<sub>2</sub>), they show a fibrous texture and contain plagioclase, biotite, amphibole and minor amounts of quartz. On the basis of their location in the Río Colorado valley, the source of this deposit could be the Chimborazo or Carihuairazo volcanoes. However, the chemical composition of the pumice (see below) suggests a link with the Chimborazo magmatic suite and points to a major explosive event associated with the Chimborazo Basal Edifice.

**4.1.2.2. Condor Palta pyroclastic flow deposits.** A sequence of block-and-ash flow deposits occurs at 8–9 km from the summit, in the valley of the Río Condor Palta, to the south of the volcano (Figs. 3, 5). This >200 m-thick sequence lies on lava flows belonging to the basal cone, particularly the Chorrera lava flow, which is dated at 76 ± 8 ka. The deposits are massive, matrix-supported with a coarse, grey, ash matrix and dense blocks of siliceous andesite (60–62 wt.% SiO<sub>2</sub>) bearing a mineral assemblage composed of plagioclase, ortho- and clinopyroxene, amphibole and Fe–Ti oxides. We associate this pyroclastic sequence with viscous lava flows and domes from the upper part of the El Castillo lava series (e.g. the Templo Machay lavas). Thick fallout deposits and moraines from the LGM period overlie the Condor Palta block-and-ash flow deposits.

**Table 2**  
Generalized chronostratigraphy showing the main eruptive stages of Chimborazo volcano.

	Volcanic units	Eruptive styles and deposits	Age	Magma composition
Young Cone (CH-III)	Holocene explosive activity	Recurrent, low-magnitude, andesitic activity (at least 7 eruptions since 7 ka)	1–8 ka	Andesitic tephra
	Río Colorado debris avalanche	Small-volume debris avalanche, deposit directed to the north	> 12–14 ka	
	Western-plateau fallout deposits	Sequence of powerful fallout deposits displaying erosional unconformities and interlayered with glacial deposits	14–35 ka	Andesitic scoriae and pumice (56–60 wt.% SiO <sub>2</sub> ) with scarce andesitic–dacitic pumice (62–64 wt.% SiO <sub>2</sub> )
	Murallas Rojas stage	Edification of the main summit: lava flows and related pyroclastic deposits		Two-pyroxene and olivine andesites (56–60 wt.% SiO <sub>2</sub> )
Intermediary Edifice (CH-II)	Río Blanco ashflow	Ash-flow deposits to the north (Río Blanco) and south (Tintatacto)	42–43 ka	
	Politécnica and Martínez stage	Edification of a mainly effusive edifice	~35–48 ka	Two-pyroxene andesites (59–63 wt.% SiO <sub>2</sub> ) and subordinate dacites (64–67 wt.% SiO <sub>2</sub> )
	Guano stage	Post-avalanche lava flows and related pyroclastic deposits (Aucacán sequence)	~60 ka	Two-pyroxenes andesites (60–63 wt.% SiO <sub>2</sub> )
Basal Edifice (CH-I)	Riobamba debris avalanche	Huge debris avalanche deposit directed to the south–east	~60–65 ka	
	Peñas Blancas ashflow	Ash-flow deposits in the Río Ambato		Biotite-bearing rhyolite 70 wt.% SiO <sub>2</sub> )
	El Castillo stage	Upper lava flows and viscous lava flow sequence (Templo Machay and Condor Palta sequence)	65–95 ka	Two-pyroxene andesites (57–60 wt.% SiO <sub>2</sub> ) and amphibole-bearing andesites and dacites (63–64 wt.% SiO <sub>2</sub> )
	Abraspungo stage	Lower lava flows	~100–120 ka	Two-pyroxene andesites (57–61 wt.% SiO <sub>2</sub> )
Carihuairazo volcano	Lavas from the lower south–east and west flanks	205–230 ka	Two-pyroxenes andesites	

#### 4.1.3. The Riobamba debris avalanche deposit (R-DAD)

Chimborazo volcano experienced a large sector collapse, whose deposit is widely exposed in the Riobamba basin, where it is delimited by the Río Guano to the north and the Río Chimborazo to the south, reaching as far as the Río Chambo, more than 35 km southeast of the volcano. Its thickness is 40 m in average, covers about 280 km<sup>2</sup> and has a bulk volume of 10–12 km<sup>3</sup>. Two main debris avalanche facies are recognized. The widespread block facies (> 80 vol.% of the deposit) is derived predominantly from the edifice lavas (Fig. 6a), whereas the least common mixed facies was essentially created by mixing brecciated edifice rock with substratum and is found mainly in distal and marginal areas. Two main lithologies have been identified in the R-DAD. The dominant group consists of porphyritic, amphibole-bearing andesites and dacites (60–63 wt.% SiO<sub>2</sub>), whereas the second group consists of dark-grey, porphyritic, two-pyroxene andesites (56–60 wt.% SiO<sub>2</sub>). In addition, scarce, glassy, prismatic jointed blocks of black two-pyroxene andesite (60 wt.% SiO<sub>2</sub>) were observed in the distal mixed facies, which might represent a juvenile component incorporated into the debris avalanche during emplacement (Fig. 6b). However, no conclusive evidence for syn-collapse eruptive activity has been found in the stratigraphic record (Bernard et al., 2008).

The debris avalanche deposit has clear surface ridges and hummocks, and internal structures such as jigsaw cracks, basal injections and shear-zone features. Substratum incorporation is directly observed at the base, namely injections of the underlying ignimbrite deposits related to the Chalupas caldera, a large volcanic structure 80–100 km northeast of Chimborazo (Fig. 1), which erupted about ~211 ka (Hall and Mothes, 2008). The volume increase during transport was estimated at 15–25 vol.% and a volume of around 10–14 vol.%

substratum was incorporated into the deposit during transport (Bernard et al., 2008). Based on these considerations, a volume of 7.2–8.4 km<sup>3</sup> was derived from the Basal Edifice. No dating has been done on the R-DAD itself. However, based on age constraints from overlying volcanic deposits (see below), as well as the fact that the sector collapse affected lavas from the Basal Edifice which are dated at ~68 ka, we infer that the collapse event occurred after this date.

#### 4.2. The Intermediary Edifice (CH-II)

This edifice was constructed on the eastern part of the avalanche depression that affected the Basal Edifice (Fig. 5). Two cone-building periods have been identified, giving rise to the construction of the Politécnica and Martínez peaks (Table 2).

##### 4.2.1. Guano stage

The first volcanic products erupted after the sector collapse that affected the Basal Edifice include the Aucacán pyroclastic sequence and the Guano lava flows. At 10–12 km to the southeast of the inferred volcanic vent of the Intermediary Edifice is a pyroclastic fan that extends from the Quebrada Aucacán to the hamlet of Cuatro Esquinas (Figs. 3, 5). The Aucacán pyroclastic sequence is composed of at least two scoria-flow deposits, whose total thickness is ~10 m. These deposits are matrix-supported, with metre-sized andesitic blocks and bombs. Juvenile fragments correspond to dark brown scoria and dense blocks of two-pyroxene andesites (58–60 wt.% SiO<sub>2</sub>). Field and aerial photo observations around the Cuatro Esquinas hamlet suggest that this pyroclastic sequence overlies the R-DAD exposed some

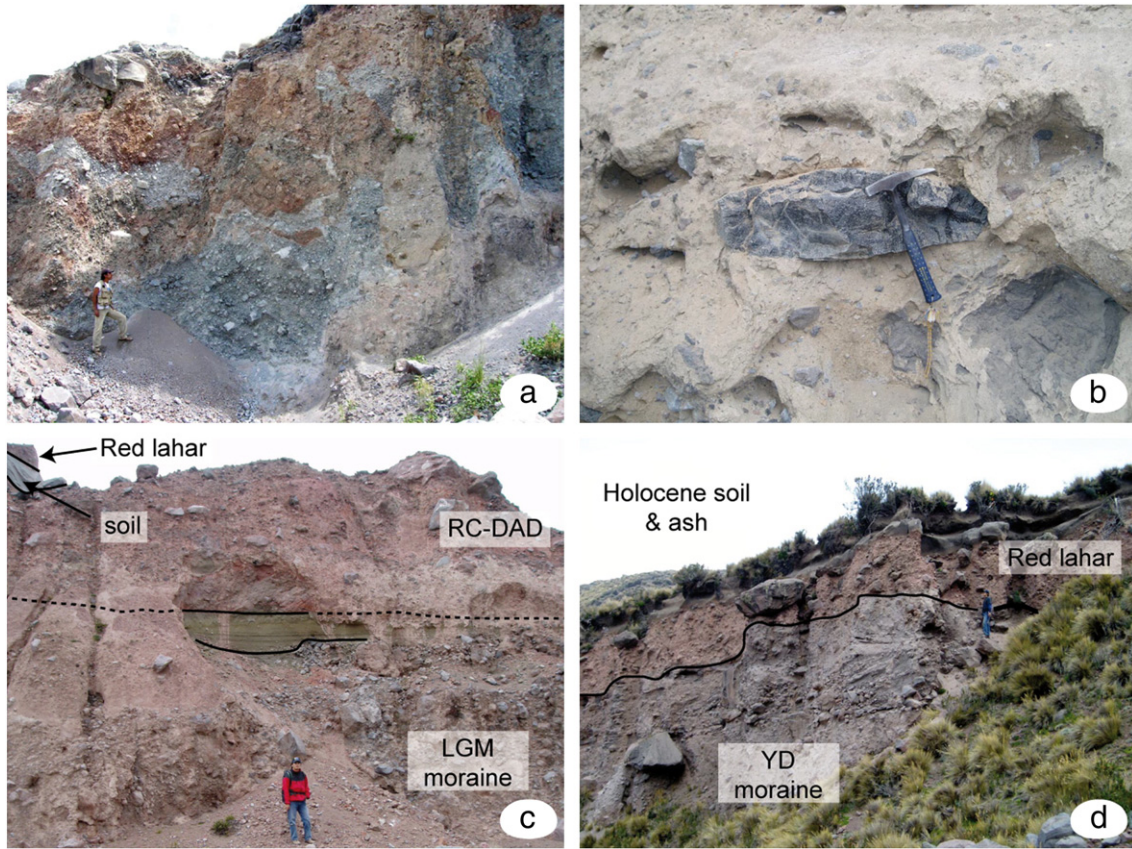


**Fig. 6.** (a) Mixed facies of the Riobamba debris avalanche deposit (R-DAD). (b) Matrix facies of the R-DAD, showing a prismatic andesitic bomb (sample CH-DB-152). (c) Polvoloma stratigraphic section (site RIO-84) showing the LGM moraines dated at > 14 ka, tephra fallout deposits, the Río Colorado debris avalanche deposit (RD-DAD) and the red lahar. (d) Huayhuayacu stratigraphic section showing a late-glacial moraine (probably associated with the 10–12 ka glacial advance) and the northern red lahar deposit.

kilometres downstream, whereas in the proximal zone these deposits are covered by the Guano lava flows.

A conspicuous (75 to 100 m-thick) lava sequence (the *Guano lava flows*) is exposed at the southeast foot of Chimborazo, forming the lower slopes of the Intermediary Edifice, and covering an area of 13–14 km<sup>2</sup>. This lava sequence has a homogeneous andesitic composition (60–63 wt.% SiO<sub>2</sub>), and bears a mineralogy composed of plagioclase, ortho- and clino-pyroxene and Fe–Ti oxides. Most of these lava flows have a length of around 8–10 km, originating from the Politécnica and Martínez peaks. However, the longest lava flow reaches 22 km, at the town of Guano, where it has a thickness of 40 m and filled a paleovalley at the northern edge of the R-DAD. These lavas, the volume of which is estimated as being 1–1.5 km<sup>3</sup>, cover the R-DAD and the Aucacán scoria-flow unit. In the proximal zone, these lavas are covered by the thick package of the LGM moraines, suggesting that these lavas are older than 33 ka. A distal sample from this lava sequence (sample RIO 5, located close to Guano, Fig. 3) yielded an isochrone age of 68 ± 10 ka (plateau age of 60 ± 11 ka). Given the large error of this sample, together with its proximity to the younger date of the pre-avalanche Basal Edifice (68 ± 4 ka, RIO-84), we assume that the sector collapse, the related Riobamba debris avalanche and the outpouring of Guano lava flows, all occurred within a short time span between ~60 and 65 ka.

#### 4.2.2. Politécnica stage

A thick lava pile that originates at the Politécnica and Martínez peaks represents the remnants of this Intermediary Edifice. The dips of the lavas below the Politécnica peak reach ~30° and the thickness of this series is around 700 m. The Martínez peak is constructed ~1 km eastwards of the Politécnica peak, and consists of a >400 m-thick lava flow sequence, the uppermost part of which consists of sub-glacial

breccias. Lavas from the Martínez peak discordantly overlie lava flows emitted from the Politécnica peak. To the southwest, these lavas have a maximum extension of 9 km from the presumed volcanic centre (Figs. 3, 5). The lavas of the Politécnica stage are mostly two-pyroxene andesites (59–63 wt.% SiO<sub>2</sub>), although rare amphibole-bearing dacites (64–67 wt.% SiO<sub>2</sub>) have also been sampled. Two lavas from the east-southeast side of the Martínez peak yield similar ages of 40 ± 8 ka and 39 ± 6 ka (CH-DB-59 and CH-DB-44, respectively, Table 1).

**4.2.2.1. Pyroclastic deposits.** The older pyroclastic deposits associated with the Intermediary Edifice crop out in the valley of the Río Blanco, 10 km to the north of the main summit. These deposits (the *Río Blanco ash-flow*) are massive and strongly eroded with a minimum thickness of ~8 m and cover a major part of the Río Blanco valley. These ash-rich deposits contain ~5 vol.% pumice and ~5 vol.% accidental lapilli and blocks, as well as abundant carbonized plant remains within the deposit. Charred twigs on the top of the deposit were dated by radiocarbon at 42,200 ± 1500 yr BP (CH-DB-120D). The deposit is covered by distal moraines associated with the LGM period.

The Tintatacto section, on the southeast flank of the volcano (CH-DB-10, Figs. 7, 8b), consists of a 5–6 m-thick sequence of at least 12 horizons of tephra fallout deposits interlayered with ash-rich, organic-poor paleosols that overlay the R-DAD. Beate and Hall (1989) found an age older than 35 ka for a pyroclastic flow deposit that overlies the debris avalanche deposit. In this study, we obtained an AMS <sup>14</sup>C age of a charcoal fragment in a 30-cm thick surge deposit that yielded an age of 42,600 ± 500 yr BP (Fig. 8b). We correlate this deposit to the Río Blanco ashflow deposit. Although these ages (~42,000–43,000 yr BP) are close to the limit of the dating method, we stress that they are in good agreement with <sup>40</sup>Ar–<sup>39</sup>Ar ages obtained on proximal lava flow samples from the Intermediary

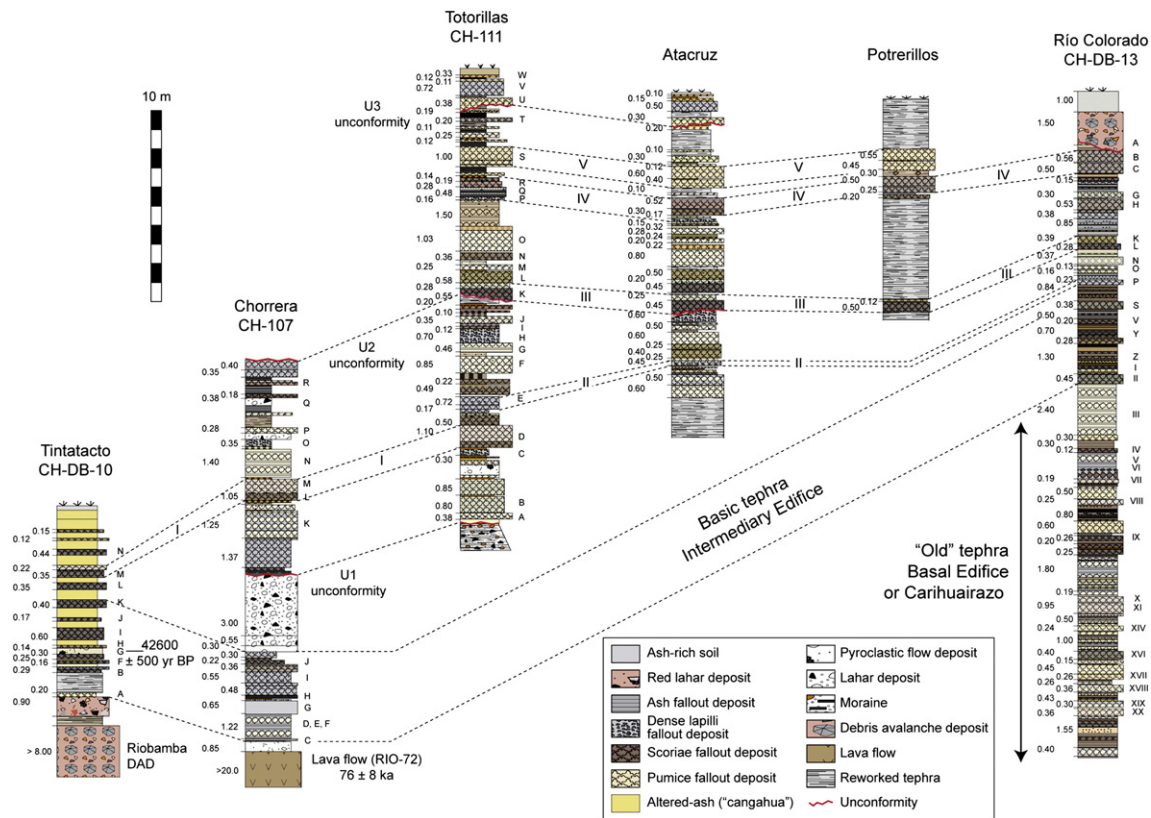


Fig. 7. Stratigraphic sections of the late Pleistocene explosive activity of Chimborazo.

Edifice (39–40 ka) and confirm that the age of the Riobamba debris avalanche should be older than 45 ka. In the Tintatacto section, tephra layers are composed of brown to black scoria clast (2–5 cm in diameter), locally with a yellowish patina, as well as multicoloured lithic fragments (5–10 vol.%) of hydrothermally altered rocks and grey lithics from older volcanic rocks. The juvenile scoria has an andesitic composition (57–60 wt.% SiO<sub>2</sub>). We correlate this section to the lower part of the fallout sequence of the southwest plateau (Chorrera section, CH-107, Fig. 7).

#### 4.3. The Young Cone (CH-III)

The youngest, and highest cone of the Chimborazo compound volcano is constructed on the remnants of the Basal Edifice (Fig. 5). We identify a main cone-building stage, which was accompanied by major explosive activity. The cone was subsequently affected by a flank collapse event (Table 2).

##### 4.3.1. Murallas Rojas stage

From the avalanche scar (i.e. the El Castillo rampart) to the limit of the glacier in the western and northern flanks, at 5500–6000 m, the younger Chimborazo cone consists of scoria-flow deposits, spatter agglutinations, and interlayered lava flows. These deposits are radially distributed around the upper part of the cone. At the Murallas Rojas site (Figs. 2b, 3), between 5400 and 5800 m in altitude on the north and northwestern flanks, we found a 5–8 m-thick sequence of pyroclastic flow deposits, associated with proximal fallout ash and scoria lapilli layers. This sequence was emplaced unconformably on lavas of the El Castillo stage of the Basal Edifice, and filled the depression left by the large sector collapse that affected this volcano. These deposits contain multicoloured, scoriaceous, two-pyroxene andesites (56–60 wt.% SiO<sub>2</sub>).

Distal pyroclastic flow deposits associated with this edifice are relatively scarce around the young Chimborazo cone. These deposits

reach distances of 7–10 km from the main summit and crop out on the western plateau, as well as on the northern and southern flanks of Chimborazo. The best exposures of this unit occur on the southern flank, in the Culebrilla Grande and Condor Palta valleys (Figs. 3, 5). Here, there is a ~20 m-thick sequence of at least four units composed of block-and-ash and scoria-flow deposits which are andesitic in composition (61–62 wt.% SiO<sub>2</sub>), and show mingling textures between light- and dark-coloured magmas. Another outcrop of this unit was found in the Río Chimborazo valley, where a 7–9 m-thick, flat-topped, valley-ponded sequence is composed of a lower, matrix-supported, block-and-ash flow unit, and an upper, indurated, matrix-supported lahar deposit. We interpret the scarcity of pyroclastic flow deposits around the cone as a consequence of the intense glacial erosion during the Late Pleistocene glaciations.

##### 4.3.2. Western-plateau tephra sequence

A 15–30 m-thick sequence of tephra fallout deposits mantles Chimborazo's western slopes and the nearby western plateau, from the Río Colorado valley in the north to the Quebrada Chorrera and Río Chimborazo in the south (Figs. 3, 5). The dispersion axis is oriented roughly to the west, covering an area of 120–140 km<sup>2</sup>, which corresponds to a minimum volume of 1.8–2.1 km<sup>3</sup>. The precise extension of this unit is unknown because the tephra was reworked during the Pleistocene glaciations, and also because tephra preservation is not favoured to the west due to the humid climate and the presence of vegetation. However, along the Guaranda-Salinas road, located ~20 km to the west of the Chimborazo summit, we found several 10–30 cm-thick tephra layers interbedded with ash-rich horizons. Despite the large area covered by these deposits, outcrops are scarce, and mostly limited to the main road cuts through the western plateau. The best outcrops occur towards the southwest foot of the volcano, at 8 km from the main summit, at the Totorillas and Chorrera sites (Figs. 3, 7). These sequences consist of at least 46 layers, each of > 10 cm in thickness (23 of these layers are > 25 cm). This tephra

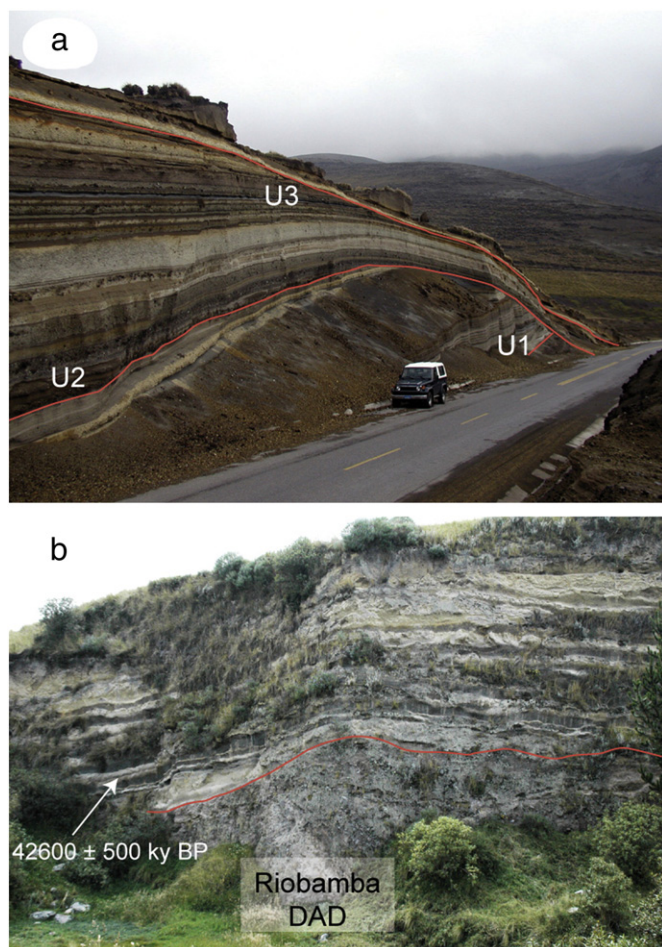


**Fig. 8.** Tephra fallout deposits of Chimborazo volcano. (a) Tephra sequence at the Riobamba-Guaranda road (Totorillas section, CH-111). The three unconformities (U1–U2–U3) are associated with glacier advances during the LGM period (ca. 33–14 ka). (b) Tephra sequence overlying the debris avalanche deposit on the eastern flank of Chimborazo (Tintatacto section, CH-DB-10). See correlations in Fig. 7.

fallout sequence comprises four sub-units which are clearly delimited by three erosional unconformities (Fig. 8a). We interpret these unconformities as glacial advances during the LGM period, roughly dated at between ca. 33 and 14 ka (Clapperton, 1990).

Based on the textural and geochemical characteristics of the tephra, we identified five key horizons in the Totorillas and Chorrera sections (Fig. 7). The lowest key horizon (I) is 105–110 cm in thickness, and occupies a median position between the first two unconformities (U1 and U2). It consists of a bicolour layer with basic andesitic brown scoria (55.3 wt.% SiO<sub>2</sub>) in the lower part, which grades to beige andesitic scoria (58.5 wt.% SiO<sub>2</sub>) in the upper part. The second key horizon (II) is a 25–40 cm layer that contains andesitic scoria lapilli (58 wt.% SiO<sub>2</sub>) with distinctive magma mixing textures. The third key horizon (III) consists of two fallout layers located just above the U2 unconformity. The lower layer (50–55 cm-thick) consists of brown andesitic (58.0–58.5 wt.% SiO<sub>2</sub>) scoria fallout with black glassy lithics that transitionally evolves to an upper normally-graded horizon of grey andesitic scoria, with a similar andesitic composition. The next key fallout horizon (IV) is a 115 cm-thick layer, located in an intermediate position between the medium and upper unconformities (U2 and U3). It consists of twin scoria layers (55.8–56.2 wt.% SiO<sub>2</sub>), brown and pink in colour, underlain by a 16 cm-thick horizon of dense, glassy lapilli of similar composition. The fifth and uppermost key horizon (V) consists of two thick (100–120 cm) fallout layers separated by a thin brown layer of fine ash. It bears vesiculated scoria

bombs reaching a diameter of 15 cm, and has an andesitic composition (60.3 wt.% SiO<sub>2</sub>).

These key horizons allow us to correlate the main stratigraphic sections around the volcano. As a result, we can correlate the Tintatacto section (samples CH-DB-10A to -10K) on the eastern flank of the volcano to the lower tephra layers beneath the U1 unconformity (Chorrera section), as well as to the tephra located around the middle position of the Río Colorado section (samples CH-DB-13S to -13Z). In addition, horizons II to V allow the correlation between the tephra sections of the western plateau (Totorillas, Atacruz, Potrerillos) and northern flank (Río Colorado). At last, we suggest that the lower half of the Río Colorado section (samples CH-DB-13III to -13XX), which contains mainly siliceous compositions, corresponds to explosive activity of the Basal Edifice and/or the neighbouring Carihuairazo volcano.

#### 4.3.3. Río Colorado debris avalanche deposits (RC-DAD)

To the north of the Young Cone, along the Ambato-Guaranda road, and forming the most recent terraces along the Río Colorado valley, we observe a conspicuous reddish-coloured, block-rich debris avalanche deposit. The thickness of this deposit at 7 km from the summit is 5 to 10 m (Figs. 6c, 9). In some places the debris avalanche deposit overlies the key horizons IV and V of the fallout sequence (Figs. 7, 9). The Río Colorado debris avalanche deposit has, in turn, been covered by the moraines of the YD period (10–12 ka, Clapperton, 1990). These deposits are associated with a small-volume flank collapse that affected the northern flank of the Young Cone, whose amphitheatre is 750 m in diameter and 1000 m high (Fig. 2b). The lower part of the amphitheatre is filled by Neo-glacial moraines and by the current glacier (Fig. 2b). The volume of the RC-DAD is difficult to estimate, because the deposit is covered by moraines and it was partially reworked into lahars. However, an estimate of the missing volume on the avalanche scar gives a volume of ~0.1 km<sup>3</sup> consistent with an area of 20 km<sup>2</sup> and an average thickness of 4 to 5 m.

#### 4.3.4. Holocene deposits

A sequence of small-volume pyroclastic deposits overlying moraines probably associated with the YD period was recently described by Barba et al. (2008). These deposits are well exposed around the eastern, northeastern and northern sides of the Chimborazo cone (Chuquipogyos, Abraspungo, and Huayhuayacu sections). At Chuquipogyos, 6 km to the east of the present summit, we found the most complete section (~4–5 m in thickness), which consists of seven slightly stratified ash layers (25–60 cm-thick), which we interpret as surge deposits; and four ash-fallout layers (2–5 cm-thick), which are interbedded with organic-rich paleosoils (Fig. 9). On the northern flank (Huayhuayacu section, Fig. 9), these deposits appear as reworked ash layers. Analyses of the juvenile lapilli fragments from the surge and fallout deposits yield andesitic compositions. Six radiocarbon dates obtained on charcoal fragments and paleosoils indicate that the eruptions occurred at quite regular intervals between about 8000 and 1000 cal yr BP.

Lahar deposits crop out over the north, west and southwest catchment areas, with an overall surface area of 8 km<sup>2</sup>. The catchment area of the Río Colorado valley contains ubiquitous, red-coloured lahar deposits, which overlie moraines of the YD period and underlie those of the Neo-glacial period. These deposits are massive, 1–2 m-thick, with a sand-rich matrix and a small quantity of decimetre- to metre-sized blocks (5–10 vol.%) of grey, black or reddish, hydrothermally altered andesitic blocks (Fig. 6d). On the northern flank, in the Huayhuayacu and Polvoloma areas, these lahar deposits are covered by a reworked, 1–2 m-thick ash layer (Fig. 9). Similar deposits were found on the western and southwestern flanks (e.g. in the Totorillas area). These lahar deposits were associated with the first two explosive events of Chimborazo during the Holocene (Barba et al., 2008).

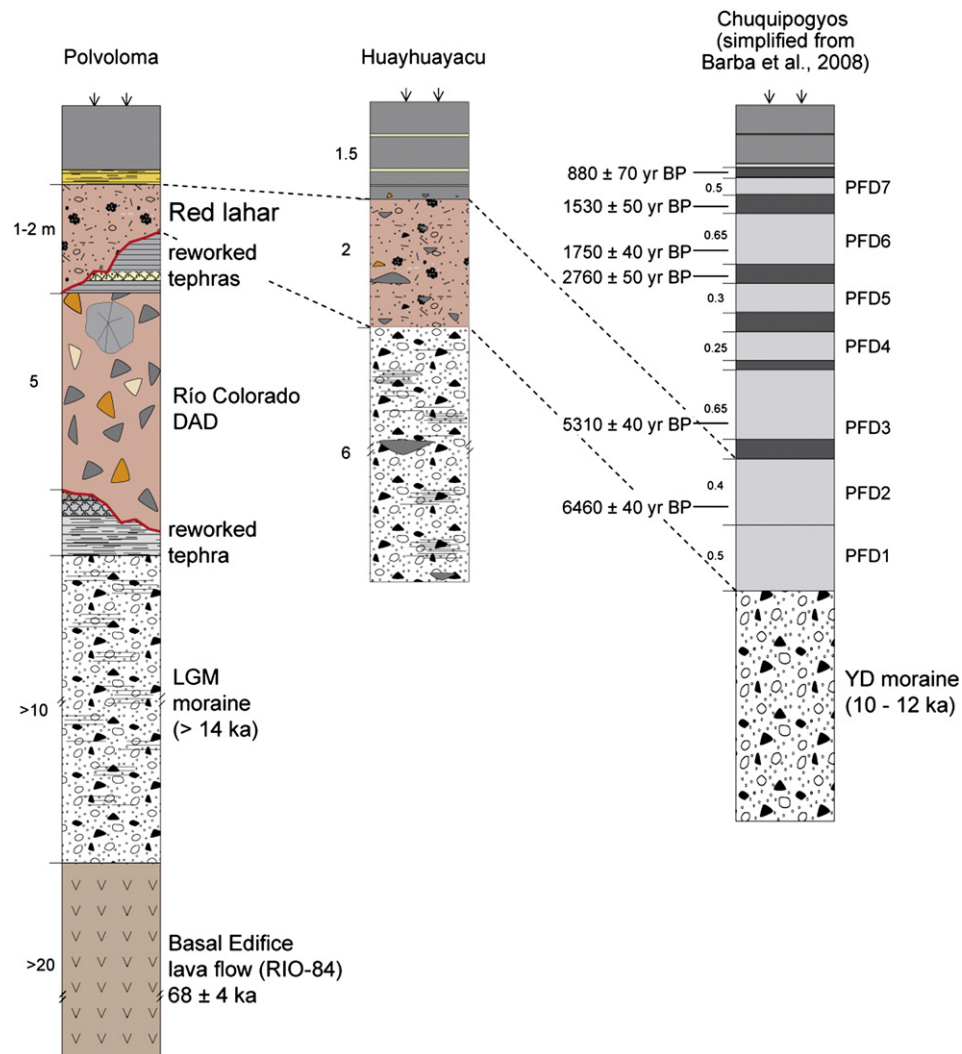
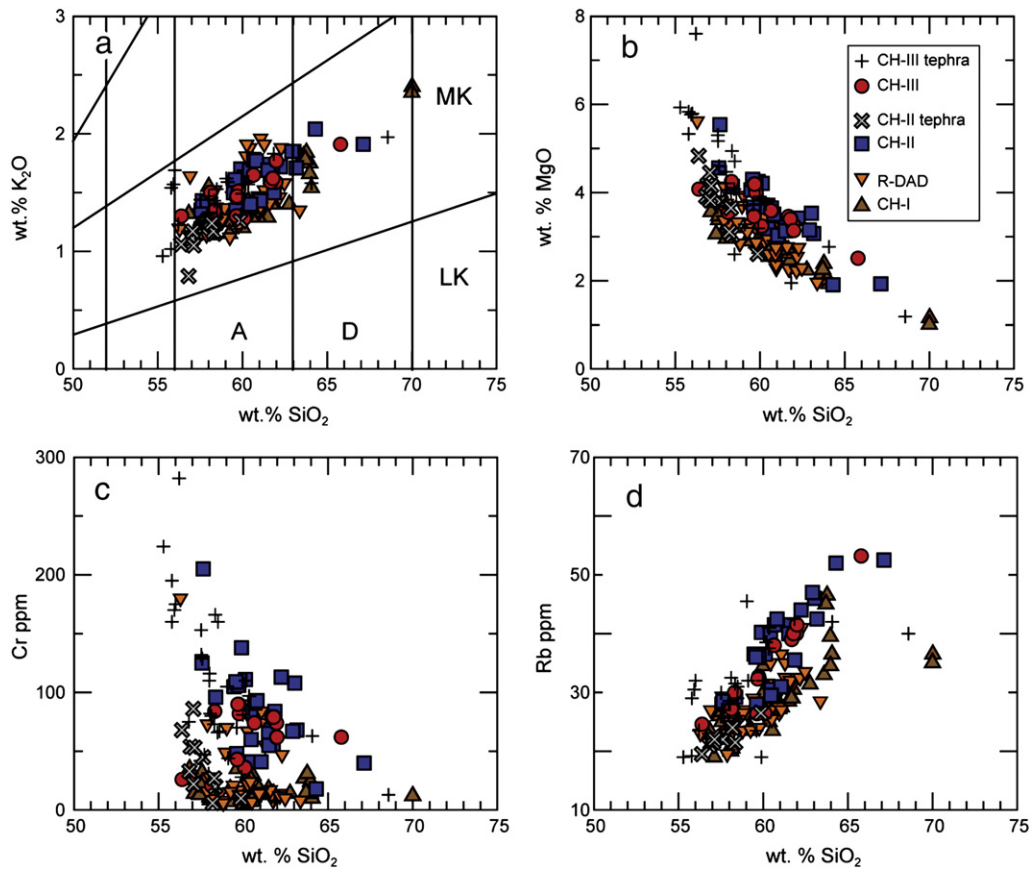


Fig. 9. Sections showing the stratigraphic relations between the RC-DAD, the red lahar deposits, and the Holocene eruptive products. PFD, pyroclastic flow deposit.

## 5. Main petrological characteristics: two distinct magmatic trends

In a  $\text{SiO}_2$  vs.  $\text{K}_2\text{O}$  plot, Chimborazo samples display a broad medium-K trend ranging from 55.3 to 70.0 wt.%  $\text{SiO}_2$  (Fig. 10), with most samples in the range of 57 to 62 wt.%  $\text{SiO}_2$ . A selected group of analyses is shown in Table 3. Basal Edifice samples are mostly andesites (57–62 wt.%  $\text{SiO}_2$ ), with rare dacitic compositions (63–64 wt.%  $\text{SiO}_2$ ), and show a mineral assemblage composed of plagioclase, ortho- and clino-pyroxene, amphibole and Fe–Ti oxides. No significant differences have been observed between the volcanic units of the Basal Edifice, however we find that the last eruptive products of the El Castillo stage (e.g. Templo Machay lavas) display silica-rich compositions and the ubiquitous presence of amphibole phenocrysts. Post-debris-avalanche volcanic units, namely those of the Intermediary Edifice (i.e. Guano lava flows and the Politécnica and Martínez peaks) and the Young Cone (Whymper summit), encompass a similar compositional range (56–63 wt.%  $\text{SiO}_2$ ) with rare dacitic samples (64–67 wt.%  $\text{SiO}_2$ ). In contrast the mineral assemblage is different from that of the Basal Edifice in that it lacks amphibole. In addition, it is worth noting that, for a similar silica content, samples from the post-debris-avalanche edifices display higher concentrations of  $\text{MgO}$  (as well as  $\text{Mg}\#$ ,  $\text{Ni}$  and  $\text{Cr}$ ) than the lavas of the Basal Edifice. We

also observe a small, but significant, enrichment in  $\text{K}_2\text{O}$ , and certain trace elements such as  $\text{Rb}$  and  $\text{Th}$ , for the post-debris-avalanche edifices compared to those of the Basal Edifice (Fig. 10). These differences have also been highlighted in Fig. 11, where selected trace element ratios (e.g.  $\text{Rb}/\text{Sr}$ ,  $\text{La}/\text{Yb}$ ) are plotted against  $\text{Mg}\#$ , which serves as a differentiation index. In summary, two different magmatic trends are defined: the Basal Edifice (CH-I); and the Intermediary Edifice and Young Cone (CH-II and CH-III). These differences in magma chemistry are useful for reconstructing the magmatic history. First, samples collected from the R-DAD form a dispersed field that mostly overlaps that of the Basal Edifice, suggesting that the sector collapse mostly affected this edifice. Second, although the tephra samples from the Young Cone (CH-III) show a broad dispersion, they mostly occur inside the field defined by the post-debris-avalanche edifices, confirming their association with the Young Cone (CH-III). In contrast, tephra samples from the Intermediary Edifice (CH-II) define a homogeneous group (Figs. 10, 11) which displays similar geochemical characteristics to the samples of the Basal Edifice. In spite of this similarity, we exclude a link between these tephra samples and the Basal Edifice because they clearly lie in a stratigraphic position above the R-DAD (Fig. 8b). The compositional signature of the CH-II tephra remains unexplained, and we propose that the change in



**Fig. 10.** Selected major and trace elements for Chimborazo samples, plotted against silica. (a) SiO<sub>2</sub> vs. K<sub>2</sub>O classification diagram. A andesites, D dacites, LK low potassium, MK medium potassium. (b–d) Variation diagrams for MgO, Cr and Rb respectively.

the geochemical signature was progressive, starting at the time of the effusion of the Guano lava flows and the associated Aucacán pyroclastic deposits.

## 6. Discussion

### 6.1. The origin of the Riobamba debris avalanche

One of the key questions concerning the Chimborazo structure concerns the stratigraphic position of the Riobamba debris avalanche deposit. According to Beate and Hall (1989) and Clapperton (1990), the sector collapse affected an intermediate edifice (now represented by the Politécnica peak), with the Martínez peak corresponding to a post-avalanche edifice. In contrast, Alcaraz (2002) proposed that the R-DAD originated from the destruction of an edifice made up of both the Politécnica and Martínez peaks. In this study we propose a new scenario, in which the semi-circular structure preserved on the western flank corresponds to an avalanche amphitheatre that affected the Basal Edifice. The argument for this interpretation is twofold. Firstly, taking into account the different sources of errors, the R-DAD has a volume of 10–12 km<sup>3</sup>, which corresponds to 7–8 km<sup>3</sup> of missing volume from the edifice (Barba, 2006; Bernard et al., 2008). This large volume does not fit with a collapse scar that only affected the Intermediary Edifice (i.e. including the Politécnica and Martínez peaks), as previously proposed. Secondly, the R-DAD and Basal Edifice samples display similar petrological signatures. The presence in R-DAD of blocks of porphyritic, amphibole-bearing andesites with prismatic jointed structures, typical of lava domes, suggests a link with the viscous lava flows and domes from the Basal Edifice (e.g. Templo Machay and Condor Palta units). In addition, for most major and trace elements, the R-DAD samples display a distribution in a

geochemical field that mostly overlaps with those of the Basal Edifice (Figs. 10, 11). Thus we propose that the eruptive history of the Basal Edifice terminated with a large sector collapse, which was responsible for the R-DAD, and not with a collapse caldera produced by a large ignimbrite eruption as was previously postulated (Kilian, 1987; Beate and Hall, 1989).

### 6.2. Chimborazo volcano development

The growth of the *Basal Edifice* (CH-I) lasted from ~120 to 60 ka. The lower eruptive products correspond to the generally effusive Abraspungo stage, characterized by thick, subhorizontal lava flows that are well exposed on the north and northeast flanks. A conspicuous unconformity marks the transition to the upper, also effusive El Castillo stage, whose age is well constrained at between 95 and 65 ka. This activity corresponds to the main cone-building stage of the Basal Edifice, whose summit reached ~6200 m asl. This basal volcano underwent major explosive phases such as the Peñas Blancas ash-flow, which was followed by the emplacement of a dome complex whose relics outcrop on the southwest flank of the volcano, namely the Templo Machay lava sequence and the Condor Palta block-and-ash flow deposits (Fig. 12a). The Basal Edifice was partially destroyed by a huge sector collapse that left a 3–4 km-wide amphitheatre (Fig. 12b). The resulting debris avalanche spread out over the Riobamba depression, has a reconstructed volume of 10–12 km<sup>3</sup>, and covers an area of 280 km<sup>2</sup> (Bernard et al., 2008).

The uppermost part of the volcanic complex, which today includes the three main summits (Whympfer, Politécnica, and Martínez), corresponds to two post-debris-avalanche edifices, which were both emplaced within the avalanche amphitheatre. Following the sector collapse that affected the Basal Edifice, the first constructional stage of the

**Table 3**  
Geochemical analyses representative of main volcanic units of Chimborazo volcano.

Edifice	Basal Edifice (CH-I)							Intermediary Edifice (CH-II)			
	Abraspungo	Abraspungo (Loma Huanuña)	El Castillo (Peñas Blancas PF)	El Castillo (Condor Palta PF)	Guano	Politécnica	Politécnica				
Volcanic stage (Unit)	CH DB 42	CH DB 15	RIO 72	CH DB 27	CH DB 24	CH DB 11	CH DB 06	CH DB 125A	RIO 5	CH DB 44	CH DB 59
Sample number											
UTM Northing	417	421	308	381	382	344	536	307	231	406	362
UTM Easting	464	439	422	410	393	424	380	436	598	451	467
Nature	lava	lava	lava	lava	lava	lava	pumice	lava block	lava	lava	lava
SiO <sub>2</sub>	57.00	64.00	57.80	60.50	59.85	63.90	66.75	61.00	61.50	59.00	62.00
TiO <sub>2</sub>	0.84	0.61	0.85	0.69	0.73	0.65	0.31	0.66	0.71	0.80	0.69
Al <sub>2</sub> O <sub>3</sub>	17.85	17.05	17.80	17.50	17.90	16.8	15.15	17.30	16.48	16.35	16.30
Fe <sub>2</sub> O <sub>3</sub> <sup>a</sup>	7.70	5.05	7.30	6.62	6.47	5.35	2.31	5.60	6.00	6.94	5.72
MnO	0.12	0.08	0.11	0.11	0.10	0.08	0.04	0.08	0.09	0.10	0.08
MgO	3.55	1.93	3.50	2.55	2.72	2.27	1.11	2.44	3.23	4.03	3.41
CaO	7.15	5.00	6.58	6.05	6.04	4.98	3.27	5.54	5.46	6.18	5.22
Na <sub>2</sub> O	4.22	4.45	4.50	4.28	4.50	4.32	4.00	4.52	4.20	4.10	4.30
K <sub>2</sub> O	1.13	1.54	1.23	1.40	1.20	1.79	2.29	1.39	1.71	1.49	1.71
P <sub>2</sub> O <sub>5</sub>	0.24	0.20	0.24	0.24	0.23	0.18	0.11	0.21	0.20	0.23	0.19
LOI	0.01	0.10	−0.01	−0.07	−0.04	0.05	4.31	0.73	0.49	0.40	−0.10
Total	99.81	100.01	99.90	99.87	99.70	100.37	99.65	99.47	100.07	99.62	99.52
Sc	15.7	8.0	13.5	11.5	11.1	11.5	4.0	10.0	13.0	14.5	12.5
V	198.0	111.0	168.0	135.0	170.0	130.0	60.0	124.0	141.0	170.0	137.0
Cr	14.0	10.0	13.0	7.5	5.0	15.0	12.0	14.0	56.0	105.0	113.0
Co	21.0	12.5	19.0	13.0	15.5	15.0	5.0	15.0	18.0	23.0	18.0
Ni	20.0	11.0	28.0	10.0	11.0	14.0	6.0	22.0	37.0	66.0	61.0
Rb	19.0	36.5	22.0	23.5	34.5	45.0	36.5	30.5	41.0	36.5	44.0
Sr	724.0	603.0	730.0	889.0	650.0	528.0	550.0	700.0	585.0	632.0	580.0
Y	16.4	11.2	13.8	16.0	13.0	15.2	4.8	11.0	14.5	11.9	10.1
Zr	101.0	80.0	110.0	102.0	113.0	170.0	42.0	100.0	155.0	125.0	125.0
Nb	4.6	5.2	4.5	4.7	4.9	5.7	1.8	4.4	5.5	4.9	4.6
Ba	461.0	702.0	600.0	600.0	548.0	775.0	646.0	652.0	750.0	690.0	730.0
La	14.5	16.0	14.3	19.5	13.2	17.4	9.5	15.0	17.8	15.6	16.1
Ce	30.5	32.0	31.0	40.0	29.5	36.5	19.5	28.5	37.0	32.0	30.5
Nd	17.4	17.0	18.0	22.0	16.5	19.0	10.3	16.2	20.0	17.0	16.8
Sm	3.7	3.5	3.7	4.3	3.6	3.9	2.1	3.1	4.2	3.9	3.4
Eu	1.1	1.0	1.1	1.1	1.0	1.0	0.5	0.9	1.0	1.1	1.0
Gd	3.4	2.9	3.6	3.8	3.0	3.3	1.5	2.7	3.6	3.1	3.2
Dy	2.9	2.1	2.5	2.8	2.4	2.6	1.2	2.1	2.5	2.2	2.0
Er	1.5	0.9	1.3	1.5	1.2	1.4	0.4	1.0	1.3	1.1	1.1
Yb	1.5	0.9	1.2	1.5	1.2	1.3	0.3	0.9	1.3	1.0	0.9
Th	3.1	3.5	2.9	3.6	2.8	4.9	1.8	2.8	4.6	3.8	5.0

*Intermediary Edifice* (CH-II) consisted of the Aucacán pyroclastic sequence and the voluminous outpourings of the Guano andesite lavas. Subsequently there was a main cone-building stage that witnessed the emplacement of thick sequences of lava flows and breccias, of which the Politécnica and Martínez peaks are the relics (Fig. 12c). The activity of this edifice turned more explosive, as evidenced by the sequence of basic tephras (Tintactaco and Chorrera sections), and culminated with at least one large explosive event, the Río Blanco ash-flow, which is dated at 42–43 ka. This edifice was highly affected by glacial activity during the LGM period, suggesting an age older than 33 ka. As a result, the Intermediary Edifice was constructed on the east flank of the Basal Edifice, and lasted 25–30 ka, from 60 to 35 ka.

The *Young Cone* (CH-III), whose vent location coincides with that of the Basal Edifice, was constructed during the main cone-building Murallas Rojas stage, and formed the Whympfer summit (Fig. 12d). This edifice was also characterized by major explosive activity contemporaneous with the LGM period (i.e. 33–14 ka). Stratigraphic sections at the northern and western flanks display a thick tephra fallout sequence interlayered with glacial and fluvio-glacial deposits associated with at least three glacier advances during the LGM period. In addition, the northern flank of the cone was affected by a flank collapse, whose deposits are exposed along the Ambato-Guaranda

highway and the Río Colorado valley. During the Holocene, Chimborazo activity was restricted to the Young Cone, and was characterized by low magnitude phreatomagmatic eruptions and associated debris flows.

### 6.3. Edifice volumes and eruptive rates

We estimated the volume of the Chimborazo edifice as follows. Using field mapping we delimited the outer boundaries of the edifice, which allowed us to calculate the basal area, as well as to reconstruct the substratum topography. A 40-m digital elevation model, obtained from 1:50 000 Ecuadorian topographic maps, was used to retrieve volcano morphometric parameters (Grosse et al., 2009). We used different models to interpolate the substratum topography, from which the volcano's height and volume were estimated. This procedure yielded a basal area of 214–222 km<sup>2</sup>, a height of 2.0–2.2 km and a volume for the whole Chimborazo compound cone of 72–83 km<sup>3</sup>. This volume does not take into account the distal deposits such as the R-DAD, the Guano lava flows and the Western plateau tephras.

Considering that the Chimborazo Basal Edifice (CH-I) corresponds to 70–80% of the whole edifice, we estimated a volume of 50–66 km<sup>3</sup> that was converted to a dense rock equivalent (DRE) volume of 40–52 km<sup>3</sup>

Young Cone (CH-III)										
Basic tephra	Murallas Rojas	Murallas Rojas	Murallas Rojas	Western plateau tephra						
CH 107I	CH DB 135	CH DB 142	CH DB 56A	CH 111A	CH 107 M	CH 107 L	CH 111E	CH 111 K1	CH 111R	CH 111S
311	393	387	287	324	311	311	324	324	324	324
419	424	419	444	384	419	419	384	384	384	384
scoriae	lava	lava	lava block	pumice	pumice (I)	scoriae (I)	pumice (II)	scoriae (III)	dense component (IV)	pumice (V)
55.80	56.00	59.50	65.25	66.90	58.00	54.20	57.60	57.40	55.00	59.20
0.85	0.86	0.77	0.51	0.37	0.80	0.88	0.86	0.85	0.74	0.76
16.85	17.40	16.30	15.44	15.65	16.45	16.55	17.00	16.80	15.50	16.50
7.95	7.65	6.50	4.51	3.40	7.03	8.30	7.12	7.00	8.00	6.40
0.12	0.12	0.10	0.07	0.08	0.11	0.12	0.10	0.10	0.13	0.09
4.78	4.05	4.10	2.49	1.16	4.67	5.81	4.18	4.42	5.75	3.70
7.40	7.55	6.70	4.62	3.34	6.50	7.40	6.66	6.40	8.20	5.65
3.93	4.06	3.97	4.25	4.55	4.08	3.62	4.23	4.26	3.50	4.08
1.05	1.29	1.45	1.89	1.92	1.28	0.94	1.31	1.45	1.52	1.54
0.24	0.33	0.22	0.16	0.20	0.22	0.20	0.26	0.27	0.25	0.20
0.37	0.56	0.43	0.40	2.57	0.43	1.39	0.63	0.39	0.65	1.14
99.34	99.87	100.04	99.59	100.14	99.57	99.41	99.95	99.34	99.24	99.26
19.6	15.5	15.0	9.5	4.7	14.9	18.6	13.7	13.5	22.8	12.6
198.0	240.0	170.0	103.0	41.0	160.0	180.0	166.0	164.0	192.0	140.0
68.0	26.0	90.0	62.0	13.0	160.0	224.0	110.0	116.0	195.0	86.0
28.0	25.0	23.0	14.5	5.0	24.0	31.0	24.0	25.0	28.0	21.0
60.0	64.0	100.0	41.0	7.0	82.0	110.0	70.0	82.0	48.0	58.0
19.5	24.6	32.7	53.2	40.0	26.0	19.0	25.0	28.5	29.0	37.5
685.0	1010.0	615.0	497.0	545.0	636.0	634.0	762.0	790.0	1000.0	610.0
14.8	14.5	13.8	9.9	11.6	12.9	13.5	12.4	13.0	15.8	13.4
102.0	107.0	130.0	125.0	147.0	112.0	98.0	117.0	125.0	109.0	132.0
4.4	5.6	5.3	4.7	5.9	4.7	4.7	5.0	5.5	4.1	5.0
550.0	850.0	720.0	755.0	880.0	610.0	505.0	690.0	730.0	615.0	680.0
13.2	21.0	16.2	15.0	19.6	15.0	13.3	17.0	18.2	26.0	18.0
28.0	42.0	33.0	29.0	38.0	31.0	27.0	35.0	37.5	50.0	38.0
16.0	22.5	18.0	14.8	19.0	17.5	16.0	20.5	21.5	27.0	20.0
3.6	4.6	3.9	2.9	3.5	3.8	3.7	4.2	4.2	5.0	4.2
1.1	1.3	1.0	0.8	0.9	1.0	1.1	1.2	1.2	1.4	1.1
3.4	3.5	3.4	2.5	2.8	3.6	3.3	3.4	3.8	3.7	3.6
2.7	2.6	2.5	1.7	2.1	2.5	2.6	2.4	2.4	2.9	2.6
1.4	1.3	1.3	0.9	1.1	1.3	1.4	1.2	1.3	1.6	1.3
1.3	1.2	1.2	0.9	1.1	1.1	1.1	1.0	1.1	1.4	1.1
2.0	3.2	3.8	5.7	4.8	2.9	2.2	3.0	3.1	6.0	4.4

assuming a bulk density of 2200 kg/m<sup>3</sup> for the entire edifice (Williams and Finn, 1985) and an average density of 2800 kg/m<sup>3</sup> for the non-vesiculated andesitic Chimborazo lava (Bernard, 2008). We added to this value the R-DAD volume (7–8 km<sup>3</sup>), which corresponds to 5–6 km<sup>3</sup> DRE (using a debris avalanche bulk density of 1950 kg/m<sup>3</sup>; Glicken, 1996). Thus, the whole volume of the Basal Edifice is in the order of 45–58 km<sup>3</sup> DRE. Given that this edifice lasted from ~120 to 60 ka (i.e. during 60 ka), its average eruptive rate was estimated to be around 0.74–0.97 km<sup>3</sup>/ka (Table 4). We stress that this output rate represents a maximum value given that the oldest Chimborazo lavas are probably buried underneath younger rocks.

Assuming that the Intermediary Edifice roughly corresponds to 17–25 vol.%, and the Young Cone represents only 3–4 vol.% of the whole Chimborazo volume, we estimated a volume of 10–18 km<sup>3</sup> DRE for the Intermediary Edifice and 2.5–4.5 km<sup>3</sup> DRE for the Young Cone. These values include the volume of the Guano lava flow sequence, and the western plateau tephra deposits (Table 4). Given that the Intermediary Edifice lasted from 60 to 35 ka (i.e. 25 ka), the estimated eruptive rate is 0.42–0.70 km<sup>3</sup>/ka. For the Young Cone we obtained a significantly lower eruptive rate of 0.08–0.13 km<sup>3</sup>/ka (for a time span from 35 ka to the present). This highlights the marked decrease in eruptive rate that occurred over the period from the construction of the

Basal Edifice to that of the Young Cone. Interestingly, Le Pennec et al. (2011) estimated a similar magmatic output rate (~0.13 km<sup>3</sup>/ka) for the last 35 ka of the potentially active Imbabura volcano in the Northern part of the Ecuadorian arc.

The eruptive rates obtained for each Chimborazo edifice contrast with the average eruptive rate calculated for the whole of Chimborazo, which is in the order of 0.5–0.7 km<sup>3</sup>/ka (assuming a whole volume of 58–80 km<sup>3</sup> DRE and a time span of 120 ka, Table 4). These values are similar to, or somewhat higher than those calculated for other Andean volcanoes such as Guagua Pichincha (0.5–0.6 km<sup>3</sup>/ka, Robin et al., 2010), El Misti (0.63 km<sup>3</sup>/ka, Thouret et al., 2001), Nevado Cayambe (0.4 km<sup>3</sup>/ka, Samaniego et al., 2005) and Puyehue-Cordón Caulle (0.42–0.51 km<sup>3</sup>/ka, Singer et al., 2008). However, the average eruptive rates estimated for Chimborazo are notably higher than the 0.04–0.2 km<sup>3</sup>/ka calculated for several silicic volcanic systems of continental arc settings such as the Central Andes (i.e. Tatara-San Pedro, Aucanquilcha; Singer et al., 1997; Klemetti and Grunder, 2008), the Cascades (Mt. Adams, Mt. Baker; Hildreth and Lanphere, 1994; Hildreth et al., 2003a) or the Trans-Mexican volcanic belt (i.e. Ceboruco, Tancitaro; Frey et al., 2004; Ownby et al., 2007).

The Chimborazo eruptive rates suffer greatly from an averaging effect, since the long repose times are also taken into account. In

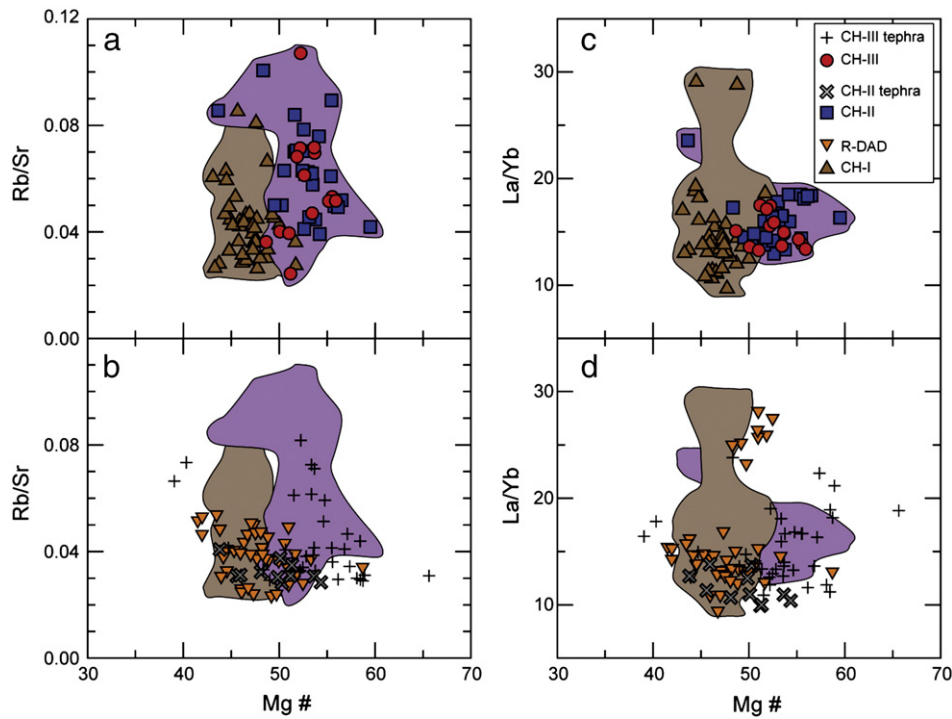


Fig. 11. Selected trace element ratios for Chimborazo samples. (a–b) Rb/Sr and (c–d) La/Yb vs. Mg#.

fact, marked eruptive rate variations have been observed at several continental arc volcanoes, such as Puyehue-Cordón Caulle (Singer et al., 2008), Mt. Adams (Hildreth and Lanphere, 1994), and the Katmai volcanic cluster (Hildreth et al., 2003b). The age constraints for the main cone-building stages of Chimborazo permit us to estimate peak eruptive rates for each edifice (Table 4). These data point to higher eruptive rates, in the range of 1.2–1.6 km<sup>3</sup>/ka (Basal Edifice), 0.6–1.1 km<sup>3</sup>/ka (Intermediary Edifice), and 0.2–0.3 km<sup>3</sup>/ka (Young Cone). These eruptive rates are similar to those obtained for the Holocene history of Cotopaxi (Hall and Mothes, 2008) and Tungurahua (Hall et al., 1999; Le Pennec et al., 2008) andesitic volcanoes. These values also confirm the progressive decrease of the magmatic output rate during the history of Chimborazo, as well as the inference that many composite volcanoes grow in “spurts” with peak eruptive rates as high as 1–2 km<sup>3</sup>/ka (Hildreth and Lanphere, 1994; Davidson and de Silva, 2000).

#### 6.4. Late Holocene eruptive activity and hazards

The newly discovered sequence of pyroclastic deposits on the north and east flanks of the Chimborazo cone were associated with the Younger Cone and crop out around the edifice at distances of more than 5 km from the present summit crater. Based on the distribution and thickness of the deposits we infer a small magnitude for these eruptions. However, the surface textures of volcanic clasts, analysed by scanning electron microscopy, indicate violent explosions due to interactions between the magma and water, which probably issued from the ice cap (Barba et al., 2008). These low-magnitude explosive eruptions contrast with those of the pre-Holocene activity dominated by major plinian events, as well as with those of the other volcanic front centres, such as Pulumahu (Papale and Rosi, 1993); Guagua Pichincha (Robin et al., 2008), Atacazo-Ninahuilca (Hidalgo et al., 2008) and Quiltoa (Mothes and Hall, 2008).

Since the last eruption probably occurred between the early part of the 5th century and the end of the 7th century (Barba et al., 2008), Chimborazo is a potentially active volcano that threatens the densely populated Ambato and Riobamba basins. Based on the

eruptive activity of the last millennia, the future eruptive activity of Chimborazo might be characterized by low-magnitude, vulcanian or phreatomagmatic eruptions associated with magma–water interactions between the andesitic magma and water provided by the large ice cap on Chimborazo. In addition, recent work carried out by a Franco-Swiss team drilled the Chimborazo ice cap in 1999–2000 (Schotterer et al., 2003), and found melted water at depths of 10–20 m inside the glacier. These water reservoirs could potentially provide a large volume of water, which could mix with eruptive products to produce far-reaching lahars. Also, given the steep slopes of the Chimborazo edifice, and its proximity to the active Pallatanga strike-slip fault system, a potential sector collapse triggered by fault activity cannot be excluded, as testified by the two debris avalanche deposits mapped in the Riobamba depression and the Río Colorado valley, respectively.

#### 7. Conclusion

The Chimborazo compound volcano comprises three edifices. The old, mainly effusive and voluminous (45–58 km<sup>3</sup> DRE) Basal Edifice (CH-I) comprises two main cone-building stages (Abraspungo and El Castillo stages), whose activity ended with a phase of dome building. This Basal Edifice was mainly andesitic in composition and developed between ~120 and 60 ka. It was affected by a huge sector collapse around ~65–60 ka that produced a large debris avalanche that spread out into the Riobamba basin, covering about 280 km<sup>2</sup> with an average thickness of 40 m and a total volume of ~10–12 km<sup>3</sup>. From ~60 ka to ~35 ka ago, the less voluminous (11–18 km<sup>3</sup> DRE) Intermediary Edifice (CH-II) grew over the east flank of the Basal Edifice, at the outlet of the avalanche amphitheatre. Activity at this volcano began with a major effusive sequence (the Guano lava flows), followed by a cone-building stage responsible for the construction of the Politécnica and Martínez peaks. This edifice was largely affected by glacial erosion, suggesting that it pre-dates the LGM period (>33 ka). Compared to lavas from the Basal Edifice, the Intermediary Edifice is characterized by more basic, Mg-rich compositions. Lastly, the eruptive activity shifted back to the west, leading

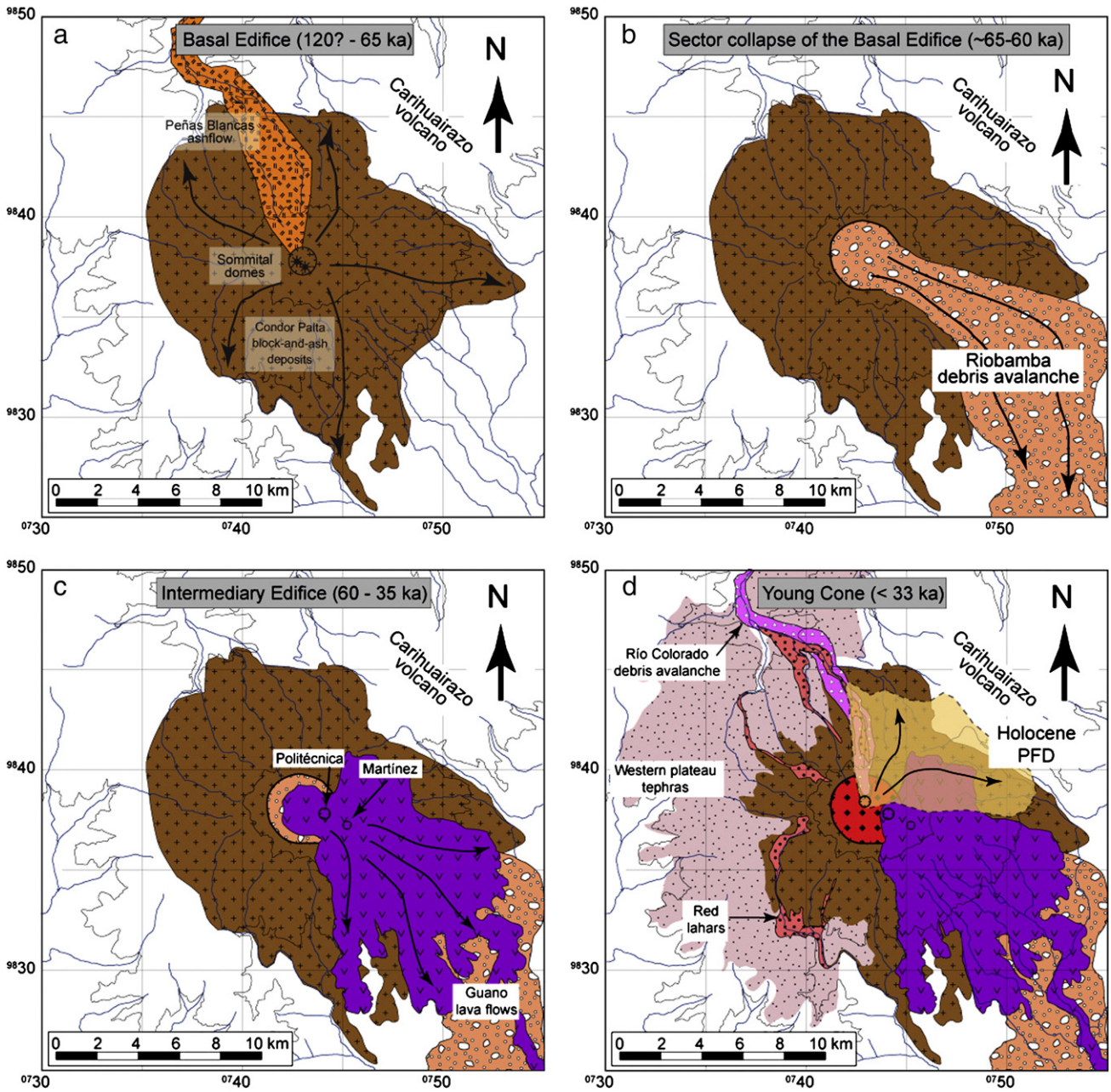


Fig. 12. Sketch diagrams showing the main development stages of Chimborazo volcano. (a) Basal Edifice and siliceous activity (ash-flow activity and domes). (b) Sector collapse affecting the Basal Edifice. (c) Post-avalanche activity and construction of the Intermediary Edifice. (d) Young Cone and sector collapse.

Table 4  
Magma eruptive rates at Chimborazo volcano.

Edifice	Units	Volume (km <sup>3</sup> )	Density (kg/m <sup>3</sup> )	Volume DRE (km <sup>3</sup> )	Total volume DRE (km <sup>3</sup> )	Lifespan	Eruptive rate (km <sup>3</sup> /ka)	Main cone-building stages	Peak eruptive rate (km <sup>3</sup> /ka)
Basal Edifice (CH-I)	Abraspungo and El Castillo stages	50.4–66.4	2200 <sup>a</sup>	39.6–52.2	44.6–58.1	120–60 ka (60 ka)	0.74–0.97	95–65 ka (30 ka)	1.19–1.55
	R-DAD	7.2–8.4	1950 <sup>b</sup>	5.0–5.9					
Intermediary Edifice (CH-II)	Politécnica stage	12.2–20.8	2200 <sup>a</sup>	9.6–16.3	10.5–17.6	60–35 ka (25 ka)	0.42–0.70	48–33 ka (15 ka)	0.63–1.06
	Politécnica and Martínez peaks								
Young Cone (CH-III)	Guano lava flows	1.0–1.5	2500	0.9–1.3	2.7–4.4	35–0 ka (35 ka)	0.08–0.13	30–14 ka (16 ka)	0.16–0.26
	Murallas Rojas stage (Whymper peak)	2.2–4.2	2200 <sup>a</sup>	1.7–3.3					
	Western plateau tephra deposits	1.8–2.1	1500	1.0–1.1					
Whole Chimborazo					57.8–80.1	120 ka	0.48–0.67		

<sup>a</sup> Williams and Finn (1985).

<sup>b</sup> Glicken (1996).

to the construction of the morphologically well-preserved Young Cone (CH-III) that is peaked by the present summit (Whymper). It consists of lava flows, pyroclastic flow deposits and a thick sequence of tephra fall deposits coeval with the LGM period (i.e. 33–14 ka). This sequence ranges in composition from basaltic andesite to dacite–rhyolite.

Taking into account the entire lifetime of Chimborazo, the average output rate is estimated at 0.5–0.7 km<sup>3</sup>/ka. However, taking into account the repose periods, a decrease in the eruptive rates is observed, from the Basal Edifice (0.74–0.97 km<sup>3</sup>/ka), through the Intermediary Edifice (0.42–0.70 km<sup>3</sup>/ka) to the Young Cone (0.08–0.13 km<sup>3</sup>/ka). We would emphasize that the peak eruption rates are markedly higher during the main cone-building stages, indicating that there are important variations in magma output rate during the lifespan of continental arc volcanoes.

Holocene eruptive activity of the Young Cone produced a succession of surge events that occurred at quite regular intervals, between about 8000 and 1000 yr ago. Since the last eruption occurred between the early part of the 5th century and the end of the 7th century, and the average time interval between the events is about 1000 yr, Chimborazo must be considered as being a potentially active volcano. The presence of a thick ice cap, its steep flanks and its position close to the populated Riobamba and Ambato basins, are all factors that increase the potential risk associated with this volcano.

## Acknowledgements

We warmly thank Joseph Cotten for carrying out the chemical analyses at the Laboratoire Domaines Océaniques, Université de Bretagne Occidentale (Brest, France). We also thank Dr. Johannes van der Plicht (U. Groningen, Netherlands) for the radiocarbon age determinations. Stimulating discussions with S. Alcaraz, B. Beate, J.P. Eissen and H. Leyrit were much appreciated. We thank the reviews of C. Siebe and an anonymous reviewer, and the editorial handling of M.T. Mangan. We also thank F. van Wyk de Vries for the English improvement of a previous version of this manuscript, and P. Ramón (IG-EPN) who kindly provide an aerial photo of Chimborazo. This work is part of an Ecuadorian–French cooperation programme carried out between the Instituto Geofísico, Escuela Politécnica Nacional (IG-EPN), Quito, Ecuador and the French Institut de Recherche pour le Développement (IRD). This is Laboratory of Excellence ClerVolc contribution n° 10.

## References

- Alcaraz, S., 2002. Etude de l'avalanche de débris du Chimborazo, 35 000 BP (Equateur). Unpublished « Mémoire d'Aptitude Géologique », IGAL Cergy-Pontoise, vol. 266, 104 pp.
- Barba, D., 2006. Estudio vulcanológico del Complejo Volcánico Chimborazo. Unpublished Thesis; Escuela Politécnica Nacional, Quito, Ecuador, 222 pp.
- Barba, D., Robin, C., Samaniego, P., Eissen, J.P., 2008. Recurrent pyroclastic flows at Chimborazo volcano, between 8000 and 1000 yr BP. *Journal of Volcanology and Geothermal Research* 176, 27–35. doi:10.1016/j.jvolgeores.2008.05.004.
- Beate, B., Hall, M.L., 1989. Informe final de Vulcanología: Tungurahua, Cotopaxi, Chimborazo. INECEL–Consultora San Francisco, Unpublished report, Parte C, 79 pp.
- Beate, B., von Hillebrandt, C., Hall, M.L., 1990. Mapa de los peligros volcánicos potenciales asociados con el volcán Chimborazo. Instituto Geofísico, Escuela Politécnica Nacional, Quito.
- Bernard, B., 2008. Étude des dépôts d'avalanches de débris volcaniques: analyse sédimentologique d'exemples naturels et identification des mécanismes de mise en place. PhD Tesis, Université Blaise Pascal, Clermont-Ferrand, 293 pp.
- Bernard, B., van Wyk de Vries, B., Barba, B., Robin, C., Leyrit, H., Alcaraz, S., Samaniego, P., 2008. The Chimborazo sector collapse and debris avalanche: deposit characteristics as evidence of emplacement mechanisms. *Journal of Volcanology and Geothermal Research* 176, 36–43. doi:10.1016/j.jvolgeores.2008.03.012.
- Clapperton, C.M., 1990. Glacial and volcanic geomorphology of the Chimborazo–Carihuairazo Massif, Ecuadorian Andes. *Transactions of the Royal Society of Edinburgh: Earth Sciences* 81, 91–116.
- Clapperton, C.M., McEwan, C., 1985. Late Quaternary moraines in the Chimborazo area, Ecuador. *Arctic and Alpine Research* 17, 135–142.
- Clapperton, C.M., Smith, M.A., 1986. Late Quaternary debris avalanche at Chimborazo volcano. *Revista CIAF* 11, 1–12.
- Davidson, J., de Silva, S., 2000. Composite volcanoes. In: Sigurdsson, H., Houghton, B., McNutt, S., Rymer, H., Stix, J. (Eds.), *Encyclopedia of Volcanoes*. Academic Press, San Diego, pp. 663–681.
- Frey, H.M., Lange, R.A., Hall, C.M., Delgado-Granados, H., 2004. Magma eruption rates constrained by <sup>40</sup>Ar/<sup>39</sup>Ar chronology and GIS for the Ceboruco-San Pedro volcanic field, western Mexico. *Geological Society of America Bulletin* 116, 259–276. doi:10.1130/B25321.1.
- Glicken, H., 1996. Rockslide–debris avalanche of May 18, 1980, Mount St. Helens volcano, Washington. Open-file report, U.S. Geological Survey, 90 pp.
- Grosse, P., van Wyk de Vries, B., Petrinovic, I.A., Euillades, P.A., Alvarado, G.E., 2009. Morphometry and evolution of arc volcanoes. *Geology* 37, 651–654.
- Hall, M.L., Mothes, P., 2008. The rhyolitic–andesitic eruptive history of Cotopaxi volcano, Ecuador. *Bulletin of Volcanology* 70, 675–702.
- Hall, M.L., Robin, C., Beate, B., Mothes, P., Monzier, M., 1999. Tungurahua Volcano, Ecuador: structure, eruptive history and hazards. *Journal of Volcanology and Geothermal Research* 91, 1–21.
- Hall, M.L., Samaniego, P., Le Pennec, J.L., Johnson, J.B., 2008. Ecuadorian Andes volcanism: a review of Late Pliocene to present activity. *Journal of Volcanology and Geothermal Research* 176, 1–6.
- Heine, J.T., 1993. A reevaluation of the evidence for a Younger Dryas climatic reversal in the Tropical Andes. *Quaternary Science Reviews* 12, 769–780.
- Hidalgo, S., Monzier, M., Almeida, E., Chazot, G., Eissen, J.P., van der Plicht, J., Hall, M.L., 2008. Late Pleistocene and Holocene activity of Atacazo–Ninahuilca Volcanic Complex (Ecuador). *Journal of Volcanology and Geothermal Research* 176, 16–26.
- Hildreth, W., Lanphere, M.A., 1994. Potassium–argon geochronology of a basalt–andesite–dacite arc system: the Mt. Adams volcanic field, Cascade Range of southern Washington. *Geological Society of America Bulletin* 106, 1413–1429.
- Hildreth, W., Fierstein, J., Lanphere, M., 2003a. Eruptive history and geochronology of the Mount Baker volcanic field, Washington. *Geological Society of America Bulletin* 115, 729–764.
- Hildreth, W., Lanphere, M.A., Fierstein, J., 2003b. Geochronology and eruptive history of the Katmai volcanic cluster, Alaska Peninsula. *Earth and Planetary Science Letters* 214, 93–114. doi:10.1016/S0012-821X(03)00321-2.
- Hughes, R.A., Pilatasig, L.F., 2002. Cretaceous and tertiary terrane accretion in the Cordillera Occidental of the Andes of Ecuador. *Tectonophysics* 345, 29–48.
- Humboldt, A., 1837–1838. Geognostische und physikalische Beobachtungen über die Vulkane des Hochlandes von Quito. *Poggendorffs Ann Phy Chem* 40, 161–93; 44, 193–219.
- Kilian, R., 1987. The development of the Chimborazo (6310 m), Carihuairazo (5106 m) and other volcanoes of Ecuador. *Zbl. Geol. Paläont. Teil I, Stuttgart*, pp. 955–965.
- Kilian, R., Hegner, E., Fortier, S., Satir, M., 1995. Magma evolution within the accretionary mafic basement of Quaternary Chimborazo and associated volcanoes (Western Ecuador). *Revista Geológica de Chile* 22, 203–218.
- Klemetti, E.W., Grunder, A.L., 2008. Volcanic evolution of Volcán Aucanquilcha: a long-lived dacite volcano in the central Andes of northern Chile. *Bulletin of Volcanology* 70, 633–650.
- Le Pennec, J.L., Jaya, D., Samaniego, P., Ramón, P., Moreno, S., Egred, J., van der Plicht, J., 2008. The AD 1300–1700 eruptive periods at Tungurahua volcano, Ecuador, revealed by historical narratives, stratigraphy and radiocarbon dating. *Journal of Volcanology and Geothermal Research* 176, 70–81.
- Le Pennec, J.L., Ruiz, A.G., Eissen, J.P., Hall, M.L., Fornari, M., 2011. Identifying potentially active volcanoes in the Andes: Radiometric evidence for late Pleistocene–early Holocene eruptions at Volcán Imbabura, Ecuador. *Journal of Volcanology and Geothermal Research* 206, 121–135. doi:10.1016/j.jvolgeores.2011.06.002.
- McCourt, W.J., Duque, P., Pilatasig, L., Villagómez, R., 1997. Geología de la Cordillera Occidental del Ecuador entre 1° y 2°S. Informe N° 3, CODIGEM-BGS, Quito, Ecuador. 68 pp.
- Meyer, H., 1907. In den Hochanden von Ecuador, vol. I. Dietrich Reimer–Ernst Vohsen, Berlin. 522 pp.
- Mothes, P.A., Hall, M.L., 2008. The plinian fallout associated with Quilotoa's 800 yr BP eruption, Ecuadorian Andes. *Journal of Volcanology and Geothermal Research* 176, 56–69.
- Owby, S., Delgado Granados, H., Lange, R.A., Hall, C.M., 2007. Volcán Tancitaro, Michoacán, Mexico, <sup>40</sup>Ar/<sup>39</sup>Ar constraints on its history of sector collapse. *Journal of Volcanology and Geothermal Research* 161, 1–14.
- Papale, P., Rosi, M., 1993. A case of no-wind plinian fallout at Pululagua caldera (Ecuador): implications for models of clast dispersal. *Bulletin of Volcanology* 55, 523–535.
- Reiss, W., Stübel, A., 1892. Reisen in Südamerika. Das Hochgebirge der Republik Ecuador. *Petrographische Untersuchungen, Vol. 1, West-Cordillere; Vol. 2, Ost-Cordillere*. Asher & co., Berlin, 358 and 356 pp.
- Robin, C., Samaniego, P., Le Pennec, J.L., Mothes, P., van der Plicht, J., 2008. Late Holocene cycles of dome growth and Plinian activity at Guagua Pichincha volcano (Ecuador). *Journal of Volcanology and Geothermal Research* 176, 7–15. doi:10.1016/j.jvolgeores.2007.10.008.
- Robin, C., Samaniego, P., Le Pennec, J.L., Fornari, M., Mothes, P., van der Plicht, J., 2010. New radiometric and petrological constraints on the evolution of the Pichincha volcanic complex (Ecuador). *Bulletin of Volcanology* 72, 1109–1129. doi:10.1007/s00445-010-0389-0.
- Rodbell, D.T., Seltzer, G.O., 2000. Rapid ice margin fluctuations during the Younger Dryas in the tropical Andes. *Quaternary Research* 54, 328–338.
- Samaniego, P., Martin, H., Monzier, M., Robin, C., Fornari, M., Eissen, J.-P., Cotten, J., 2005. Temporal evolution of magmatism at Northern Volcanic Zone of the Andes: the geology and petrology of Cayambe volcanic complex (Ecuador). *Journal of Petrology* 45, 2225–2252.
- Sauer, W., 1971. *Geologie von Ecuador*. Gebrüder Borntraeger, Berlin-Stuttgart, Berlin. 316pp.

- Schotterer, U., Grosjean, M., Stichler, W., Ginot, P., Kull, C., Bonnaveira, H., Francou, B., Gäggeler, H.W., Gallaire, R., Hoffmann, G., Pouyaud, B., Ramirez, E., Schwikowski, M., Taupin, J.D., 2003. Glaciers and climate in the Andes between the Equator and 30° S: what is recorded under extreme environmental conditions? *Climatic Change* 59, 157–175.
- Singer, B.S., Thompson, R.A., Dungan, M.A., Feeley, T.C., Nelson, S.T., Pickens, J.C., Brown, L.L., Wulff, A.W., Davidson, J.P., Metzger, J., 1997. Volcanism and erosion during the past 930 ky at the Tatara–San Pedro complex, Chilean Andes. *Geological Society of America Bulletin* 109, 127–142.
- Singer, B.S., Jicha, B.R., Harper, M.A., Naranjo, J.A., Lara, L.E., Moreno-Roa, H., 2008. Eruptive history, geochronology, and magmatic evolution of the Puyehue-Cordón Caulle volcanic complex, Chile. *Geological Society of America Bulletin* 120, 599–618. doi:10.1130/B26276.1.
- Thouret, J.C., Finizola, A., Fornari, M., Legeley-Padovani, A., Suni, J., Frechen, M., 2001. Geology of El Misti volcano near the city of Arequipa, Peru. *Geological Society of America Bulletin* 113, 1593–1610.
- Whymper, E., 1892. *Travels among the Great Andes of Ecuador*. Charles Scribner's Sons, New York. 456pp.
- Williams, D.L., Finn, C., 1985. Analysis of gravity data in volcanic terrain and gravity anomalies at subvolcanic intrusions in the Cascade Range, USA, and at other selected volcanoes. In: Hinze (Ed.), *The utility of regional gravity and magnetic anomaly maps*: Society of Exploration Geophysicists, pp. 361–376.
- Winter, T., Avouac, J.P., Lavenu, A., 1993. Late Quaternary kinematics of the Pallatanga strike-slip fault (Central Ecuador) from topographic measurements of displaced morphologic features. *Geophysical Journal International* 115, 905–920.